Joint Centre for Mesoscale Meteorology, Reading, UK

Simulation of Orographic Rainfall in South Wales with UM Version 5.2

JCMM Internal Report No 136

NWP Scientific Paper 70

July 2002

H W Lean

Met Office Joint Centre for Mesoscale Meteorology Department of Meteorology
University of Reading PO Box 243 Reading RG6 6BB United Kingdom
Tel: +44 (0)118 931 8425 Fax: +44 (0)118 931 8791
www.metoffice.com

Designed and produced by the Met Office © Crown copyright 2002 02/0392
Met Office and the Met Office logo are registered trademarks

1. Introduction and Aims

Orographic rainfall is an important aspect of the significant weather which a high resolution model will need to correctly represent. This report describes preliminary results from orographic rain case study reruns of the UM at version 5.2. A particular interest is the representation of the seeder feeder mechanism which occurs in particular in the warm sectors of depressions and is thought to account for a large proportion of the orographic rainfall in the UK (Bader and Roach 1977, Browning 1980). In this report a simplified analysis of the seeder-feeder mechanism is first described leading to a numerical model of the problem. Results are then described from UM version 5.2 with a 12km gridlength and a comparison is given with the simplified numerical model of the seeder-feeder process. The effect of smoothing the orography in the 12km model along the lines being proposed for the operational model is discussed. A comparison is then made with the UM in its hydrostatic version (4.5). Finally there is discussion of results of similar reruns of the model at high resolution (2km) and global resolution (60km).

2. Analysis of Seeder-Feeder Mechanism and Simplified Numerical Model

2.1 Description of Seeder-Feeder Mechanism

The seeder-feeder mechanism of orographic rain is illustrated schematically in Figure 1. When air is forced to ascend up a hill the resulting condensation produces low level water cloud. In many cases there is a distinct Low Level Jet (LLJ) which defines the level at which this cloud peaks. On its own this water cloud might be expected to produce rain by autoconversion. The rate of the process, however, is usually too slow to produce significant rain in the time it takes the air to cross the hills. The seeder-feeder mechanism involves some "seeder" rainfall falling into this orographic cloud. This "seeder" rain is typically generated by larger scale ascent causing condensation - often of ice by the Bergeron-Fineisen mechanism. This rainfall increases by accretion in the lower level ("feeder") cloud and results in significantly higher rainfall at the ground than would result from either the feeder rain or the seeder cloud alone.

This view of the seeder-feeder mechanism is a simplified ideal which is be used for the analysis described in this section. In practice, however, it is likely to be complicated by a number of factors:

(a) The seeder and the feeder cloud may not be separate

(b) The seeder rainfall may be also enhanced by the orography (by locally enhancing the ascent at the higher levels).

(c) The melting level might be down in the region of seeder rainfall or even in the LLJ region. This will complicate the situation since ice processes will come into play. In addition advection of snow by the wind is likely to be more significant than the advection of rain due to the difference in fall speed.

(d) The advection of the rain by the wind may be significant. Simple calculations show that this effect may be important on the scales of order 10km which may be significant in high resolution models.

These factors and their influence on the resulting rainfall will be discussed further in later sections. An analysis of this ideal seeder-feeder mechanism has been carried out and is described in the next section. This leads to equations which can not be solved analytically so a resulting numerical model is described in the section 2.3

2.2 Analysis of ideal seeder feeder mechanism.

The simplified analysis which has been carried out takes account of only three processes:

1. The condensation of vapour to form the "feeder" cloud
2. The accretion process by which rain falling from above depletes the cloud and increases itself as it falls.
3. The advection of the feeder cloud

Throughout it is assumed that the temperature is above freezing, i.e. no ice processes are included. Rain is assumed to fall vertically.

The analysis is carried out considering the lower portion of the atmosphere in the LLJ region of height h. At the top, z=h, a prescribed, seeder, rainrate is assumed which is assumed to be a constant, P_h, in this section (although it is allowed to vary when fitting to the UM results as described in section 4). Assuming the three terms described above the variation of water cloud, q_{cl} (kg/kg), along a level, is given by

$$U\partial q_{cl}/\partial s = C - A \qquad (1)$$

Where U is the wind velocity at that level, C is the condensation rate and A is the accretion rate.

In order to calculate the condensation it is assumed that the air is saturated so that any ascent will cause condensation. Since the air of interest here is relatively close to the ground the ascent is initially represented simply by $U\alpha$ where α is the gradient of the orography (when it comes to matching this model with UM runs the vertical velocity is instead imposed to match that in the model). The condensation term is then simply approximated by $C_0U\alpha$ where C_0 is the condensation per m which the air is lifted. In the cases of interest this can be calculated to have a value $C_0 \approx 1.8\text{x}10^{-6}\text{m}^{-1}$.

The accretion rate is calculated by making the same assumptions as the UM mixed phase precipitation scheme (Wilson and Ballard 1999) i.e. that the rainfall drop size distribution of the rain entering the top of each level is given by a gamma distribution. Integrating over the distribution gives the simple result that $A=(dq_{cl}/dt)_{acc}=q_{cl}A_0P^{0.68}$ where $A_0=0.14\ \text{kg}^{-0.68}\text{m}^{1.36}\text{s}^{-0.32}$.

Putting these together with (1) gives

$$\partial q_{cl}/\partial s=\alpha C_0 -(q_{cl}/U)A_0P^{0.68} \qquad (2)$$

which gives the variation of q at one level given the precipitation rate at that level, P(s,z). In general both α and P may be functions of s. The second component of the analysis is to link together the different levels by writing down how the rainrate is changed by the accretion. Considering the fluxes of rainfall leads to the simple conclusion that the rate of change of precipitation rate with height is given by

$$\partial P/\partial z = -\rho A \qquad (3)$$

where A is the accretion rate as before and ρ is the density of air (~1 kgm^{-3})

For a given $P_h(s)$, $\alpha(s)$, $q_{cl}(0)$ and U(z) one would hope to solve these equations to obtain $q_{cl}(s,z)$, the cloud water distribution, and P(s,0) the surface rainfall rate. In general this has to be done numerically and this is the subject of the next section.

Some useful insight can, however, also be obtained by considering the solution in the special case of $P_h(s)$, $\alpha(s)$ both being independent of s for s>0 – i.e. the ascent up a half infinite long upslope (where the source of moisture never runs out) starting with $q_{cl}(0) = 0$, $U(z)=U_0$. In this case it is expected that the solution will reach a steady state after a certain distance which means that the left hand side of (2) will become zero. This leads immediately to expressions for the limiting values of q_{cl} and P.

$$q_{cl\infty} = U_0 \alpha C_0 P^{0.68}/A_0 \qquad (4)$$

For the precipitation rate (3) becomes $\partial P_\infty/\partial z = -U_0 \alpha \rho C_0$ which may be integrated trivially to give the result

$$P_\infty(z) = P_h + U_0 \alpha \rho C_0 (h-z) \qquad (5)$$

This is simply stating the obvious fact that in equilibrium all the moisture condensed in the layer between the level z and the top of the model, h, must come out as rainfall In order to calculate some sample values some typical numbers may be assumed i.e. $U_0=20ms^{-1}$, $P_h=0.5$ $mmhr^{-1}$ and also $\alpha=0.02$ which corresponds to a rise of 300m over a distance of about 15km (which is roughly the slope of the upslope in the case described in later sections). (In this report although the constants etc are given for SI units the quoted rainfall rate values are converted to $mmhr^{-1}$ from $kgm^{-2}s^{-1}$). In this case the equilibrium cloud water value on the top level, $q_{cl\infty}$, works out to 2.1×10^{-3} kg/kg. The total enhancement of rainfall from (5) in a depth of 1.5km works out to around 4.0 $mmhr^{-1}$.

It is also important to have an idea of the distance scale over which these equilibrium values would be reached. For the top level because P_h is assumed independent of s (2) has a simple analytic solution which is an exponential relaxation of the value of q_{cl} from an assumed value of zero at s=0 up to the equilibrium value given by (4). The e-

folding length of this exponential, i.e. the length scale for the equilibrium to be established is given by:

$$\lambda_h = (U_0/A_0)P_h^{-0.68} \qquad (6)$$

For the same numbers λ_h has a value of around 60km. As discussed in section 2.4 this implies that it would take considerably further for the values to settle to equilibrium. The implication is that the equilibrium approximation is not likely to be very useful on the top level since in the UK at least upslopes of hills will tend to be shorter than or of the same order as 60km. It is important to remember, however, that λ_h is only the value on the top of the feeder region. Further down (where it would be more useful to know!) there is no simple analytic solution because the precipitation rate falling from above depends on distance. It is therefore necessary to consider numerical solution of these equations and this is done in the next section. In addition useful progress can be made with scale analysis and this is described in section 2.4.

2.3 A numerical seeder-feeder model

This section describes the essential results from numerically solving (2) and(3) for the semi infinite hill case described in the last section. The simple model described is also compared to UM results in section 4.

In order to solve (2) and (3) numerically the hill is divided into a number of points in the s direction (200 in the case shown here) and N levels in the vertical (15 at 100m intervals in this case). The method used is to integrate (2) along the top level (once again assuming q_{cl} =0 at s=0) using the prescribed values of the precipitation falling into the top of the top level P_N (constant in this section but not necessarily for the model). Then (3) is used at each point along the level to calculate P_{N-1} . These values are then put into (2) to integrate for q_{cl} on level N-1 and so on right down the model until the surface rainrate is obtained.

Results are shown in figures 2 (a) and (b) using (except for the gradient, α) the values quoted in the last section. In the left hand half of the figures (0-100km) a constant gradient, α=0.02, is assumed. In the right hand half the gradient is set to zero. This means that the simulation is of a long upslope followed by a flat plateau in order to see how the rain rate and cloud water grows and then decays. Figure 2(a) shows the cloud water values. The top curve which is the top of the model appears to be correctly tending towards the equilibrium value described in the last section (2.1×10^{-3} kg/kg) with about the correct e-folding scale (~60km) in the upslope region below 100km. Lower levels equilibrate more quickly – this is the subject of the next section. Above 100km where the land is assumed level the cloud water decays away with approximately the same distance scale. In this simple model the cloud water values monotonically fall as the levels get lower due to the increased rainfall accreting out the cloud. In the real case there would be a maximum at some level reflecting a maximum value of condensation. Figure 2(b) shows the corresponding rainfall rates. As would be expected from the cloud water curves the surface rainrate equilibrates more quickly than the 60km value derived for the top level.

These results are clearly of limited applicability to the real world for numerous reasons. In particular although representative values of various parameters, in particular the gradient of the hill, have been chosen in the case described below the upslope was only about 15km long rather than 100. The purpose of the model presented in this section is to illustrate the theory. In section 4 results will be presented from this simple model with various input parameters chosen to be more directly applicable to the case of interest.

2.4. Scale Analysis

The steady state solution for a half infinite slope presented in equations (4) and (5) above raise the issue of whether progress may be made with scale analysis to see if there is some kind of universality about the curves on various levels. The values of q_{cl} and P may clearly be scaled by the equilibrium values given by (4) and (5). As far as the distance goes a characteristic distance scale of the problem is the distance, L, in which the condensation term alone would produce the equilibrium amount of q_{cl}. This condition may be written $L\alpha C_0 = q_{cl\infty}$. Substituting (5) into this leads to the result

$$L(z) = (U_0/A_0)P_\infty(z)^{-0.68} \qquad (7)$$

It is noticeable that on the top level L(h) is the same as λ_h, the relaxation length of the analytic exponential solution. On the levels below this analytic solution doesn't hold but L still gives a distance scale. If L(z) is calculated for the numbers discussed in section 2.2 L(z) varies from 60km at the top to about 15km near the ground.

Figures 3(a) and (b) show qcl and rainrate curves from the model described in the previous section normalised both in value ($q_{cl\infty}$ or $P_\infty(z)$) and distance (L(z)). The normalisation of the qcl values has been carried out by simply dividing by $q_{cl\infty}$. In the case of rainrate there is the complication of the imposed rainrate at the top, P_h, which is added to all the rainrates produced by the seeder-feeder process. Hence the normalised P plotted is $(P-P_h)/(P_\infty(z)-P_h)$. The curves which were normalised used the same numbers as previously i.e. as in figure 2 up to 100km but extended to 400km with the same value of α=0.02. There are no "universal" curves as such in the sense that the curves don't lie on top of each other. However in all cases the curves approach 1.0 at about the same rate relative to s/L and are within 10% of 1.0 by s/L ~3. This shows that, although the exact solution is not known the distance scale is a useful concept – L gives a length scale for the seeder-feeder process to reach equilibrium. An important conclusion from this is that even at the bottom of the model one would expect to take approximately 45km (using these figures) for the precipitation and cloud water values to reach their equilibrium values. Many hills in the UK will have upslopes about this length or shorter so the equilibrium values will not be a good approximation.

2.5 Integrated Rainfall up Slope.

In practice it is often of interest to consider the total precipitation produced integrated along the model along a finite upslope of length, l, with total height $l\alpha$=H. In the limit where the upslope is long compared to the equilibration length i.e. l>> L equilibrium is established and integrated rainfall along the slope is clearly proportional to the

value of P_∞ which is proportional to α and therefore H, the height of the hill. However in the other limit where l<< L then the solution becomes a linear increase (as can be seen in figure 2(b)). The integrated rainfall along the slope then becomes proportional to $l^2\alpha$ i.e. lH which is the volume under the hill rather than the height. These two limiting cases are very relevant to the discussion on the effects of smoothing orography in section 4.4.

2.6 Drift of Rain

One effect which has not been included so far is drift of the rain in the wind. This is fairly easy to include in the simple numerical model described in section 2.3 and so its impact is briefly discussed here. In order to include this effect an assumption has to be made about the vertical fall rate of the rain. Since elsewhere in the model the gamma distribution of rainfall is used the vertical fall rate is taken to the average value over the gamma distribution which gives

$$V_{av} = V_0 P^{0.22} \qquad (8)$$

Where V_0=17.5ms^{-1} . The fall speed is lowest where the rainfall rate is lowest and so in these regions the drift of rain will be more significant. The effect of including drift of rain is shown in figs 3 (c) in the case shown before of a 100km upslope followed by a plateau. Although the precipitation rate reaches the same value as equilibrium is approached towards the end of the 100km upslope the equilibrium is attained somewhat more slowly in the run including drift of rain The effect of the drift is to redistribute the rainfall up the slope on distance scales of around 10km. So models running with higher resolution than this should include this effect. Currently the UM (as described in the rest of this report) does not.

3. Selection of case

The initial modelling work in this project was carried out on a case of orographic rainfall over the Pennines on 5th-6th Nov 2000. This case was of practical interest because it caused a great deal of flooding. The situation was, however, complicated from the analysis point of view because the melting level was relatively low – in fact it was in the middle of the LLJ region. For this reason it was decided to look for a case which didn't have this problem. The case eventually chosen took place during the early part of this work on the 29th Nov 2001 and was of orographic rainfall over South Wales. Figure 4 shows the analysis chart for 0Z on the 29th which shows the UK embedded in a south westerly flow in a warm sector. Scrutiny of the operational mesoscale model output for that day showed a good deal of orographically enhanced rain over the South Wales mountains. The melting level was up at around 2.5km which is well above the LLJ which was centred at 800m. There was therefore reason to believe that the problems with the melting layer seen with the Pennines case would be avoided here.

The problem with this case is that, although it appears to be a relatively simple seeder-feeder example, it is not very representative. The great majority of cases looked at had the melting level lower as in the Pennines case. The follow up to this work (not described in this report) involves looking at a more representative (but harder to analyse) case.

4. Reruns with UM vn5.2 12km models

4.1 Description of model

The simulations which will be described in this section were carried out with version 5.2 of the UM. The runs were carried out on the standard 0.11 degree (approx. 12km) UK mesoscale horizontal domain using the G3 New Dynamics set of 38 levels. Since the operational model at the time of the case was version 4.5 the model had to be run by converting an operational UK mesoscale model dump from version 4.5 to 5.2. The boundary conditions were obtained by running the global model at version 5.2 which required first converting an operational global model dump to version 5.2. (Results from the global model are discussed in section 7 below). The model was run with the standard 3B mixed phase precipitation scheme which includes the advection of snow but not of rain. The runs described in the next section used the same orography dataset as the operational (version 4.5) run but runs with smoothed orography are described in section 4.4

4.2 Overview of results

The overall distribution of surface pressure and rainfall from these runs were very similar to those seen in the operational runs. There were differences in the orographic rainfall which are the subject of section 5 which compares results from the hydrostatic and non-hydrostatic models. Figure 5 shows an overview of the model large scale rainrate and mean sea level pressure at 12Z. Figure 6 shows the rainrate and the orography at 11 and 12Z. There is good evidence from this picture that the area of rainfall over South Wales is orographic in origin – it doesn't move between the two times (unlike the band of more general lighter rain in which it is embedded) and it is on the upslope of the mountains. (Similar effects can be seen on the upwind sides of the mountains in Central and North Wales as well as on Exmoor).

The analysis of the mechanism of this rainfall in the model must take into account two separate elements. Firstly there is the dynamical response of the model to the orography, in particular the amount and distribution of vertical velocity produced. Secondly there is the response of the microphysics to this ascent, in particular the amount of cloud and rainfall which is produced. (This is partially addressed by the analysis of the seeder-feeder mechanism which was presented in section 2). In both of these elements account needs to be taken of the fact that the orography is only an enhancement mechanism. Even without the orography there is a large scale ascent leading to some rainfall from the structure of the front which is crossing the region.

In order to assess how this model produces the rainfall enhancement some cross sections are now discussed which are taken along the line marked in figure 6 i.e. approximately along the wind crossing from the Bristol Channel up the slope into the South Wales mountains.

Figure 7 shows the cross section of the along section component of the wind with the vertical velocity field shown as contours. The wind field shows that there is a clear LLJ centred about 500m above the surface. The vertical velocity structure shows a corresponding maximum at a similar but somewhat lower level. The vertical velocity field can be seen more clearly in the cross sections in figure 8. These cross sections are twice as long as that in figure 7 having been extended an equal distance to the SW

(i.e. the left of the cross section) and show a comparison between 11 and 12Z. This has been done to illustrate which features are not moving to the right with the large scale flow and therefore are likely to be due to the orography. Above the maximum the value of vertical velocity drops off much more rapidly than the horizontal wind. The expected dynamical response to flow over orography is discussed in many textbooks (see for example Holton 1972). In an ideal case with sinusoidal orography and $U(z) = U_0$ independent of height the resulting stationary waves in the perturbation vertical velocity field, w', can be written

$$w' = U_0 h_0 \exp(i(kx+mz)) \qquad (8)$$

Where k is the horizontal wavenumber of the waves ($2\pi/\lambda$) which is the wavenumber of the sinusoidal orography, m is the vertical wavenumber and h_0 is the amplitude of the sinusoidal orography. It can be shown that the dispersion relationship in this case is given by

$$U_0^2 = N^2/(k^2+m^2) \qquad (9)$$

where N is the square root of the Brunt Vaisala frequency ($N^2 \equiv (g/\theta)d\theta/dz$). Simply rearranging this expression leads to the expression for the vertical wavenumber.

$$m = (N^2/U_0^2 - k^2)^{1/2} \qquad (10)$$

This makes it clear that there are two regimes. For short wavelength ($kU_0>N$) hills m is imaginary and so the disturbance is evanescent in the vertical. For longer wavelengths ($kU_0<N$) m is positive and so the waves propagate upwards with a tilt upstream. The transition between these two regimes occurs when $kU_0=N$. In this case at low levels N varies between 0.01 and 0.02 s^{-1} which corresponds to a transition wavelength of λ =6-12km. Given that the model gridlength here is 12km (which obviously implies gridscale waves of 24km) one would expect that, in this model, all resolved scales would give waves of the propagating type. The response to a single hill, as in this case, will be a superposition of the responses to the fourier frequencies present. . In the long wavelength limit (k small) (10) reduces to $m=N/U_0$. If the values of N and U_0 used above are put in the first node (i.e. $\lambda/4$) is expected to be between 1.5 to 3km from the ground which agrees well with the height of the maximum in the vertical velocity field near the ground. Shorter wavelength waves would be expected to have their first node further up which may account for the disturbance extending higher.

Turning to the microphysics, figure 9 shows the cross sections of water cloud and ice cloud. There is significant water cloud generated by the orography at and above the level of the LLJ. Only about half the total would appear to be orographically generated, however, since cloud with about half the peak value pre-exists on the left hand side of the cross section which must result from the large scale structure. The ice cloud although it is clearly advecting eastwards also has a peak value in a position related to the orography. Comparison with the vertical velocity field (figure 8) implies that this peak is related to a peak in the vertical velocity at that level. Figure 10 shows the rainfall and snowfall rates at the two different times. Once again there is a broad peak in the snowfall rate which appears to be tied to the position of the orography. At 11Z the actual peak value is further west. The relationship between the upper level precipitation rate and the surface rainfall rate is explored in the next section with the help of the seeder-feeder model.

4.3 Comparison to seeder-feeder model

In order to further analyse the rainfall enhancement seen in the 12km UM vn5.2 runs described above they have been compared to the numerical seeder-feeder model described in section 2.3. In this case the numerical model was 3km deep with 30 levels and 100 points long. An attempt was made to simulate the enhancement along the cross section shown in figure 7. The rainfall rate at the top of the model was taken from the UM run as was the vertical distribution of U and qcl(0), the value of qcl at the inflow (left) side of the cross section. The vertical velocity was also set up to be as close as possible to that seen in the model by adjusting the values of α taking account of the imposed values of U. This model was therefore simply a test of the enhancement due to the accretion of rainfall in the low level water cloud.

The results of this at 11 and 12Z are shown in figure 11. The agreement with the UM enhancement of surface rainfall is generally good confirming that the seeder-feeder mechanism is responsible. At 11Z (as mentioned in the last section) the broad western (left in figure) peak in the "seeder" precipitation rate at the top of the seeder-feeder model is well to the west of the main peak in the surface rainrate. The position of the main peak in surface rainrate is primarily determined by the position of the low level water cloud. This is confirmed by the observation, figure 12, that if the seeder-feeder model is run with the same vertical velocity profiles but a constant precipitation rate at the top the resulting surface rainrate has a broad peak similar, but somewhat to the east of, that seen in the 11Z simulation. In contrast at 12Z there is a sharper peak in the precipitation rate at the top of the model which is coincident with the low level water cloud. The peak rainfall at the ground is still coincident with the maximum of the low level cloud, as would be expected. The presence of the peak in the "seeder" precipitation serves to make the peak at the ground sharper.

The implication of these results is that the approximate position and the overall magnitude of the rainfall at the ground is determined by the position of the low level "seeder" cloud. However the exact magnitude and distribution of the surface rainfall also depends on the details of the upper level "seeder" precipitation. In later sections it is, indeed, found necessary to take account of the upper level precipitation in explaining the differences in orographic rainfall between models.

4.4 Comparison of smoothed and unsmoothed orography.

The UM run discussed above was carried out using the same orography dataset as used in the current (version 4.5) operational mesoscale model. In this section a comparison is made to a run carried out using the smoothed orography dataset which it is proposed to use when the version 5.2 model becomes operational. A comparison of the two datasets over Wales is shown in figure 13. The rationale behind filtering the orography is that the model can not properly handle features on the gridlength scale and so it is sensible to remove forcing on those scales. There is a risk that forcing on the incorrectly resolved scales will generate incorrect structure which due to nonlinearity will damage the representation on resolved scales.

Figure 14 shows a comparison between model runs using the two sets of orography. The hourly accumulated rainfall over Wales is shown as block plots with each block representing a model gridpoint. It is immediately clear from this figure that the total amount of orographic rainfall in both South Wales and Snowdonia does not change

very much between the two models. In order to investigate this in more detail the top two frames of figure 15 show the same data zoomed in over the region of orographic rain over South Wales. The average accumulation of rainfall over the domain shown has been calculated for the two runs and, as shown in table 1, only changes by about 1.5%. There is, however, some redistribution of the rainfall. The lowest frame of figure shows the sign of the difference between the rainfall in the two runs. As would be expected the unsmoothed run has higher rainfall actually on the upslope but this is compensated by lower rainfall around.

In order to analyse the reason why these two runs give very similar rainrates figure 16 shows similar fields but for the 500m vertical velocity fields. The average vertical velocity on the domain shown changes from 0.1228 m/s in the unsmoothed orography run to 0.1217m/s in the run with smoothed orography (i.e. a 1% change). However the maximum vertical velocity (table 1) changes by more like 5% - as with the rainfall there is significant redistribution of the vertical velocity. Considering first the large scales in the problem the fact that the domain average vertical velocity doesn't change very much implies that the total distance the air rises is the same between the runs. The upslope is likely to be of order or longer than the equilibration length, L, discussed in section 2.4. Hence the equilibrium limit discussed in section 2.5 applies that the total rainfall should be proportional to the height the air is raised. This means that the total rainfall up the slope would be expected to be the same between the runs, as indeed seen. As far as the small scale variations which are present in the unsmoothed orography go, these can be regarded as a series of sinusoidal perturbations on the large scale orography structure. The small scale variations are in the short limit discussed in section 2.5 i.e. the total rainfall should be proportional to the volume under the mountain. This is zero for the short range perturbations which explains why adding them causes a redistribution of rainfall rather than a change in the total. An interesting corollary is that the fact that this analysis appears to work suggests that the small scale perturbations on the orography seem to add to the large scale ones in a linear fashion.

A final point is that the rationale given for filtering the orography at the start of this section i.e. that the model may not handle the short range scales correctly may or may not be right. There would need to be comparison with observations to determine whether the distribution of the rainfall on short scales is more correct in the runs with smoothed or unsmoothed orography.

5. Comparison of vn4.5 to vn5.2 models at 12km

The 29th November case was also run at 12km with version 4.5 of the model which contained the old, hydrostatic, dynamic core. The interest in this comparison is partly theoretical in order to assess the affect on orographic enhancement of using a hydrostatic model compared to a non-hydrostatic one. This is also of great practical interest since the hydrostatic model is currently in use as the operational mesoscale model so this comparison gives an idea of the likely changes in the orographic rainfall when the new model becomes operational.

Figure 17 shows a comparison of the hourly accumulated rainfall between the two models. It is clear that the different model makes quite a large difference. Looking at the South Wales orography the hydrostatic model has the peak rainfall further up the slope and the impression is that there is less overall rain in this model. More details of

the comparison can be seen in table 1. In particular the average accumulated rain over the same area as discussed in the last section is 10% less in the hydrostatic model than in the non-hydrostatic one. Unfortunately there is no satisfactory way to verify which of these models is closer to the truth. Verification will form part of the future work on this project.

In order to understand in more detail the difference between the models some cross sections are now discussed. The first issue to be addressed is the difference in position in the peak of the rainfall relative to the hill. Figure 18 shows a cross section of vertical velocity and snow rate. As discussed in section 4.2 the non-hydrostatic model has an upstream tilting maximum in the vertical velocity field. This maximum is much more upright in the hydrostatic model as would be expected from theoretical considerations of a hydrostatic wave. From equation (10) it is clear that the vertical wavenumber, m, tends towards a constant value for long horizontal wavelengths (k small). In this limit rather than being tilted the wave vector becomes vertical. This long wavelength situation represents the hydrostatic limit since the vertical velocity is forced very slowly by the orography compared to the Brunt Vaisala frequency.

Apparently as a result of the changed position of the upper level vertical velocity feature the maximum in the snow rate field is further downstream (up the slope) in the hydrostatic model. Figure 19 allows comparison of the snowfall rate with the cloud water and rainfall rate fields. The lower part of the cloud water maximum does not change position but the upper part is again tilted differently corresponding to the vertical velocity tilt. The maximum surface rainfall rate moves up the slope as a result in the change of position of the maximum of upper level snowfall rate and the change in the position of the upper parts of the "feeder" cloud. Due to the smaller change in the water cloud position the surface rainfall maximum does not move up the slope as far as the maximum in the "seeder" precipitation at higher levels.

The other issue is the overall smaller amount of rain in the hydrostatic model. From the cross sections in figure 19 and the values in table 1 the reason appears to be that there is more seeder precipitation in the non-hydrostatic model. This is consistent with this model having more ascent at altitudes of around 3km as shown in figure 18. Perhaps counterintuitively the hydrostatic model, which has less low level ascent, has *more* cloud water in the LLJ region. This is presumably a result of there being less water accreted out due to less precipitation falling from above.

6.Vn5.2 reruns at 2km.

6.1 Introduction

This section discusses the reruns of this case with 2km gridlength with version 5.2 of the model. The grid used was 300 x 300 gridpoints covering a large area of the SW UK. These runs were carried out using operational T+1 (i.e. 1Z) 12km post IAU dumps reconfigured to the 2km grid. The boundary conditions were obtained from a intermediate 4km model. The 2km model was run with both a 2km orography data set and also with the same dataset used in the 12km runs interpolated to 2km resolution. The latter was done to allow a direct comparison with the 12km runs by using the same orography – it also allows the comparison of smoothed and unsmoothed orography in a similar way to that discussed in section 4.4 In the next section the results from the 2km model with 12km orography are compared to those from the

12km model. In section 6.3 the 2km runs with 2km orography are described and compared to the other runs.

6.2 Comparison of 2km reruns with 12km orography with 12km reruns

Comparison of the 12km model with the 2km model with 12km orography should give a clean comparison of the two models without the complication of higher resolution forcing in the 2km model. This 2km model is clearly primarily of interest to enable greater understanding of the model since, in practice, one of the main benefits of using a 2km model is expected to be the representation of higher resolution orography.

Figure 20 shows the comparison of 11-12Z rainfall accumulation between the 2km and 12km runs. As would be expected from the use of 12km orography in the 2km run there is relatively little structure on scales below 12km. If the rainfall amounts are considered (as made clearer in figure 21 where the 2km data has been averaged up to 12km) then it is apparent that over the area of South Wales of interest there is less rain in the 2km model. If the same area is considered as in figure15 there is approximately 20% less rain in the 12km model. It is noticeable, however, that the opposite appears to be the case over North Wales – i.e. there is *more* rain in the 2km model over this area. If an average is calculated over a similar region encompassing most of the area of enhancement there is approximately 20% more rain in the 2km model. Although this study is not particularly concerned with the North Wales area it is of interest to ask why there appears to be a difference in this case.

In order to analyse the difference between the runs cross sections are once again considered. Figure 22 shows a comparison of the vertical velocity and snowfall rate on a cross section across the S Wales mountains. In addition values of various relevant parameters can again be seen in table 1. There are two distinct effects of interest in changing the model resolution:

1. The most obvious point is that the vertical velocity maxima in the LLJ region is significantly larger in the 2km run. This is expected from the fact that the orography in use in these runs is the unfiltered 12km orography. It is expected (see for example Lean (2001)) that models will attenuate features which are smaller than about 5 gridlengths which is 60km in the 12km model. Hence it is not surprising to see that the 2km model has a 50% larger peak in the low level vertical velocity than the 12km model with the same orography. The corresponding cloud water concentration maximum in the LLJ region (not shown in a figure) changes from 0.000332 kg/kg in the 12km model to 0.000400 kg/kg in the 2km model. This increase on its own would be expected to lead to higher surface rainfall in the 2km model through increased seeder-feeder enhancement.

2. There is a second effect which is shown by the snowfall rate field in figure 22. Although the peak value of the snowfall rate is somewhat larger in the 2km run if a larger part of the cross section is considered the average value is larger in the 12km run. This can be seen in the figure by looking at the 0.8 contour for example which is significantly larger If the area average value of the snowfall rate is calculated at 3400m (i.e. the level of maximum snowfall rate in most places) as shown in table 1 the value is approximately 18% greater in the 12km run than in the 2km one. This reflects the fact that the vertical velocity at these levels is larger

on average which can also be seen in the figures. This would generally be expected since if the 12km model is aliasing some of the short scale vertical velocity onto the scales it can resolve there will be more longer wavelength features which will be expected to extend further upwards (some of the shorter wavelengths in the 2km model might be short enough to be evanescent in the vertical). On its own this effect should lead to more rainfall in the 12km model since there is more "seeder" rainfall.

These two effects act in opposite directions but in the South Wales case shown in figure 22 the second dominates and there is more rainfall in the 12km model. Figure 23 shows the corresponding fields for a cross section across Snowdonia where there is more rain in the 2km model as described above. Although a detailed analysis has not been carried out it appears that the effect of the steeper and shorter upslope in this case is to make effect 1. above dominate over effect 2 in this case. For example the maximum values of cloud water in this section is 0.000475kg/kg in the 2km model and 0.000375kg/kg which is a larger difference than in the South Wales case. The overall message from this is that the effect of changing from a 12km to a 2km model even without changing the orography is complicated and the sign of the change of the rainfall depends on the details of the situation.

6.3 2km runs with 2km orography

This section considers the 2km runs with 2km orography and compares them with 2km runs with (unsmoothed) 12km orography and the 12km runs. Figure 24 compares the 12 and 2km orography datasets used. As would be expected considerably more detail appears in the 2km dataset with higher peaks and a number of previously unresolved valleys appearing. Figure 25 shows the 11-12Z accumulated rainfall from the 2km models with these two datasets - the 2km orography run contains much more short scale structure which to some degree can be associated with new features appearing in the orography. In order to compare the totals the same fields are plotted in Figure 26 averaged up to 12km with the 12km model also for comparison. In both North and South Wales the 2km orography run has more rainfall than that with 12km orography. This means that the rainfall total from the 2km run with 2km orography is closer to the results of the 12km run than the 2km run with 12km orography in South Wales but even further away in North Wales. The area average values over the South Wales domain can also be seen in table 1. It would be hoped that the 2km model with 2km orography is the most reliable model in this study. The fact that the average accumulated rainfall is significantly different from the 12km model casts doubt on the reliability of the 12km model. This question needs to be addressed by verification against observations to find which model is, indeed, closest to the truth. Another question raised by these results is why the rainfall totals change significantly in going from 2km to 12km orography with the 2km model when, as described in section 4.4, the 12km model gave very similar results with smoothed and unsmoothed orography. The explanation is that the 12km orography contains only spatial frequencies of 24km wavelength and longer waves. This is more drastic smoothing than is applied in the vn5.2 12km dataset and it is therefore not surprising that the rainfall totals are somewhat reduced.

Another aspect of the runs with 2km orography is illustrated in figures 27 and 28. Figure 27 shows the vertical velocity fields at 720m and it is immediately obvious that there appears to be much more wave activity in the run with 2km orography than in that with 12km orography. If these fields are animated it is found that the wave like

structures are stationary which implies that they are generated by the orography. Although in the 2km orography run significant orography (e.g. the mountains of South Wales) appears to generate wave activity the waves are not limited to downstream of these regions and seem to appear just about everywhere over land. Figure 28 shows a cross section along a line traversing the South Wales mountains. This confirms that both the upslope and the downslope of the mountains are generating very significant waves in the 2km orography run to a much greater degree than in that with 12km orography. These waves, presumably gravity waves or wake vortices, do not have a large impact on the precipitation field (although some of the stronger features can be seen weakly in the rainfall field) but are an important difference between the models with the two orography datasets.

7. Global Model

This section presents results of running this case with the global configuration of the version 5.2 model. This was done using the version 5.2 standard jobs so the set up should be as close as possible to what is intended to be operational. These runs were carried out using both the smoothed orography due to become operational along with the version 5.2 model and the original, unsmoothed, orography which is used operationally in version 4.5. The global model has a horizontal gridlength of approximately 60km at the latitude of the UK. There is practical interest in how well the global model handles orographic precipitation over the UK from the forecasting perspective and, in particular, in the question of whether the change to smoothed orography will change the rainfall totals significantly. Figure 29 compares the orography in this model to that in the 12km model. The representation of the orography in Wales in the global model consists of a just few gridpoints and there is no distinction between the mountains of North, South or Central Wales as there is in the 12km model. The highest peaks are around 300m in the unsmoothed global model and 200m in the smoothed compared to about 500m in the 12km model. Bearing in mind that the model is not expected to represent correctly features on the gridlength scale it might be expected that the representation of the orographic rainfall will be rather poor in the global model. The smoothed orography is put into the model in order to avoid problems with instabilities caused by sharp changes in the orography. When the run with unsmoothed orography discussed here was carried out it actually failed an hour or so after the times shown here, presumably as a result of these problems (although presumably not over Wales).

The sea level pressure fields from both global runs (not illustrated) look very similar to that of the 12km model confirming that the overall evolution is very similar (the boundaries of the 12km run are, of course, derived from the global but the starting analyses different due to the mesoscale assimilation). Figure 30 shows the 11-12Z accumulated rainfall for the global model with smoothed and unsmoothed orography and also, for comparison, the same data for the 12km model area averaged to the global grid. All the models have a general area of frontal rain crossing the SW of the UK. The point of interest is the amount of enhancement of this rainfall that there appears to be due to the orography of South Wales. Even when averaged up to the global grid this is very obvious in the 12km model. There appears to be some enhancement in the global run with unsmoothed orography although compared to the 12km run the peak has moved south into the Bristol Channel (this is probably a consequence of the positioning of the very poorly resolved orography). The run with smoothed orography might have enhancement in a similar position but it is smaller

and much harder to distinguish from the general frontal rain. It is also noticeable there is evidence of a rain shadow downwind in the 12km and unsmoothed orography global but not in the smoothed orography global. This confirms the impression that there is much less orographic enhancement in the run with smoothed orography. If the total accumulated rainfall is calculated over the global gridpoints covering most of the area of interest in S Wales it is found that the total is approximately 20% smaller in the run with smoothed orography compared to the run with it unsmoothed. The unsmoothed orography run itself has about 25% less rain than the 12km run by this measure. It is also notable that, in contrast to the 12km model, there appears to be very little sign of orographic enhancement over Snowdonia in either global run although there is more sign of a rain shadow in the unsmoothed orography run.

In conclusion, it appears that the representation of the orographic rainfall in this case is very poor in the global model because the mountains themselves are very poorly represented being of a horizontal size comparable to the gridlength. In the light of this fact it is not surprising that there is also found to be a good deal of difference between the runs with smoothed and unsmoothed orography. In the unsmoothed orography run most of the orographic rain is probably being produced by (incorrect) response to orography on gridlength scales which are not present in the smoothed orography run.

8. Conclusions and Future Work

8.1 Conclusions

The main conclusions of the work on this case are listed below:

- Running the case with UM version 5.2 at 12km resolution shows that the orographic enhancement is consistent with the seeder-feeder mechanism in that it agrees with a simple numerical seeder-feeder model. This simple model takes into account only condensation of water ("feeder") cloud, advection of water cloud and the depletion of the water cloud by accretion of rainfall falling from above.

- The orographic enhancement is sensitive to both the amount and distribution of "feeder" cloud at lower levels and also the amount and distribution of the "seeder" upper level precipitation which is determined by the upper level vertical velocity. This upper level vertical velocity is a combination of large scale effects and also localised maxima and minima due to waves propagating upward from the orography.

- A comparison of UM version 5.2 at 12km using the standard 12km orography dataset (as used operationally at version 4.5) with the same model using a smoothed orography dataset (proposed for use at version 5.2) shows some redistribution of orographic rainfall but totals over regions of hills unchanged to 1% or so. This is understandable because the large scale orography is the same in the smoothed and unsmoothed cases (as witnessed by the fact that the average vertical velocity over the upslope is very similar between the runs). This is expected to determine the total rainfall because the seeder-feeder effect will reach equilibrium on these scales. The small scale orographic perturbations present in the unsmoothed data are expected to lead only to redistributions of the rainfall given that the seeder-feeder effect will not reach equilibrium. The apparent correctness of this analysis implies that the short scale perturbations have a linear impact on the orographic flow. Nothing can be said from this analysis about

whether the redistribution caused by the small scale features is handled correctly by the model.

- A comparison of UM version 5.2 (non-hydrostatic) at 12km with equivalent runs at version 4.5 (hydrostatic) shows that the rainfall is about 10% less in total and the peak is moved further up the slope in version 4.5. This is consistent with the more upright waves expected over the orography in a hydrostatic model

- A comparison of a 2km model (using 12km orography) with the 12km model shows that in some areas the rainfall totals over orography are smaller in the 2km model, as in the South Wales area of interest. However in other areas, such as the North Wales mountains, there is more rainfall in the 2km model. In both cases the differences between the two models are of order 20%. The 2km model will tend to represent higher maxima of the vertical velocity on the upslope (increasing the "seeder" cloud). It will also tend to have the vertical velocity maximum extending to lower altitudes (due to the shorter spatial scales represented) which will decrease the "feeder" upper level precipitation. These two effects are opposite in effect on the seeder-feeder precipitation and so the sign of the difference between the two models will depend on the circumstances.

- The 2km model with 2km orography produces enhanced orographic precipitation (of order 10%) compared to the 2km model with 12km orography. This is expected since 2km to 12km orography represents much more drastic smoothing than that discussed above for the 12km model. However the 2km model with 2km orography still produces about 15% less rain than the 12km model in the South Wales area. This casts doubt on the accuracy of the 12km model. There need to be observational studies to check which is closest to reality. The 2km model with 2km orography produces far more wave type activity than the 2km model with 12km orography but this seems to have very little impact on the precipitation totals.

- The global (60km) model has been run for this case using both the unsmoothed and smoothed orography. It is found that in both these cases there is significantly less (around 25% in the current case) orographic rain than in the 12km model. In addition the run with smoothed orography has about 20% less rain over the area of orography than the run with unsmoothed orography. These results are seen because the orography of South Wales is inadequately represented at 60km resolution and most of the structure there is appears at the gridlength scale.

- The simplified numerical seeder-feeder model has also been run including drift of rain. The results show a significant redistribution of the rainfall on scales of about 10km which implies that models with higher resolution than this should include a prognostic rain variable in order to represent these effects correctly.

8.2 Future work

- It is important to try to find ways to verify the model results against observations. For example it has been found that moving to a non-hydrostatic model will move the position of the orographic rainfall but it is not clear if that is in better agreement with reality. The problem is that radar data is not reliable over mountains (Nimrod uses model calculated enhancements so the use of that for verification would be circular). Other possibilities are rain gauge data (possibly

climatological) and river flow data. Looking at other cases where there are more data might help (see, for example, the point below).

- Look at a new case – probably 5th March 2002 in Scotland. This might help with verification since can look at rain shadow downstream of mountains.
- Continue to look at resolution issues with the current model. Would like to look at effect of increasing the resolution to 1km and increasing the vertical resolution (currently there are not very many levels in the region of interest for the seeder-feeder process so it is possible that increasing this will have a big impact).
- Try running the models including prognostic rain when this becomes available.

References

Bader M.J. and Roach W.T., " Orographic Rainfall in Warm Sectors of Depressions" Quart.J.R.Met. Soc. **103** pp269-280 1977.

Browning K.A. "Structure, Mechanism and Prediction of Orographically Enhanced Rain in Britain" Chapter 3 of "Orographic Effects in Planetary Flow" GARP Publications Series no 23 WMO 1980.

Holton J.R. (1972) "An Introduction to Dynamic Meteorology" Third edition Academic Press

Lean H.W., "A Study of the Effects of Horizontal and Vertical Resolution in the New Dynamics representation of FASTEX IOP16" JCMM Internal report 132/NWP Scientific Paper 64 October 2001

Wilson, D. R., Ballard, S. P., 1999.
"A microphysically based precipitation scheme for the UK Meteorological Office Unified Model". Quart. J. Roy. Meteor. Soc., **125**, 1607-1636.

	12km, 12km unsmoothed orography	12km, 12km smoothed orography	12km, Hydrostatic unsmoothed orography	2km, 12km unsmoothed orography	2km, 2km unsmoothed orography
Accum. rainfall area averaged mm	2.51	2.55	2.20	2.07	2.14
Max. rainfall rate mm/hr	3.56	3.65	3.28	4.41	5.00
Area averaged 3300m snowfall rate mm/hr	0.793	0.813	0.714	0.647	0.668
Max. snowfall rate mm/hr	1.17	1.27	1.04	1.26	1.06
Max. vertical velocity m/s	0.232	0.221	0.205	0.350	1.13
Max. cloud liquid water 10^{-4}g/g	3.32	3.52	3.72	4.00	4.70

Table 1. Overview of 12 and 2km runs. The accumulated rainfall is from 11-12Z and all other quantities are at 12Z. Area averages are over the area of the South Wales mountains shown in figure 15. Maximum values are on the cross sections in figures 7 onwards (i.e. not at any specific level). The entry for the average 3300m snowfall rate in the hydrostatic model is actually at a slightly higher level (3460m) due to the levels being different in that model.

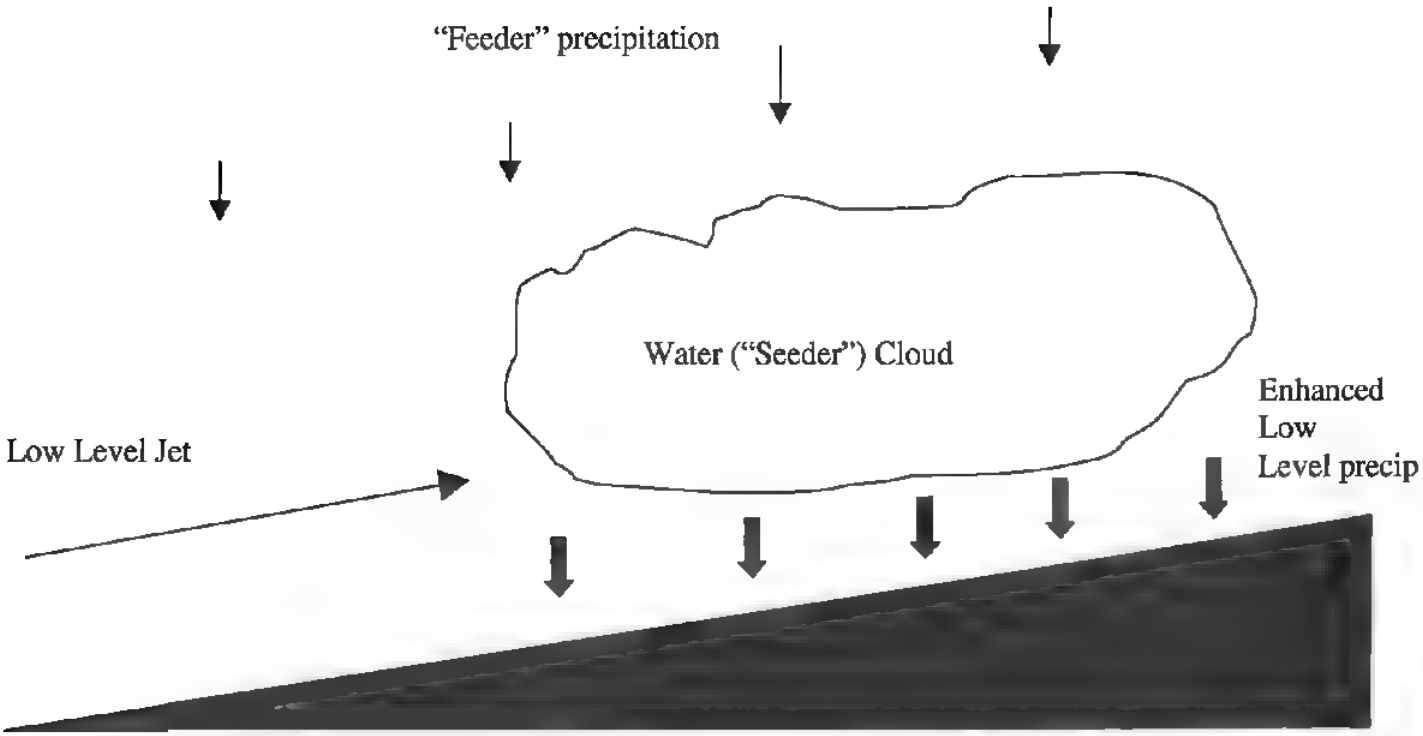

Figure 1 Schematic of Seeder-Feeder Process

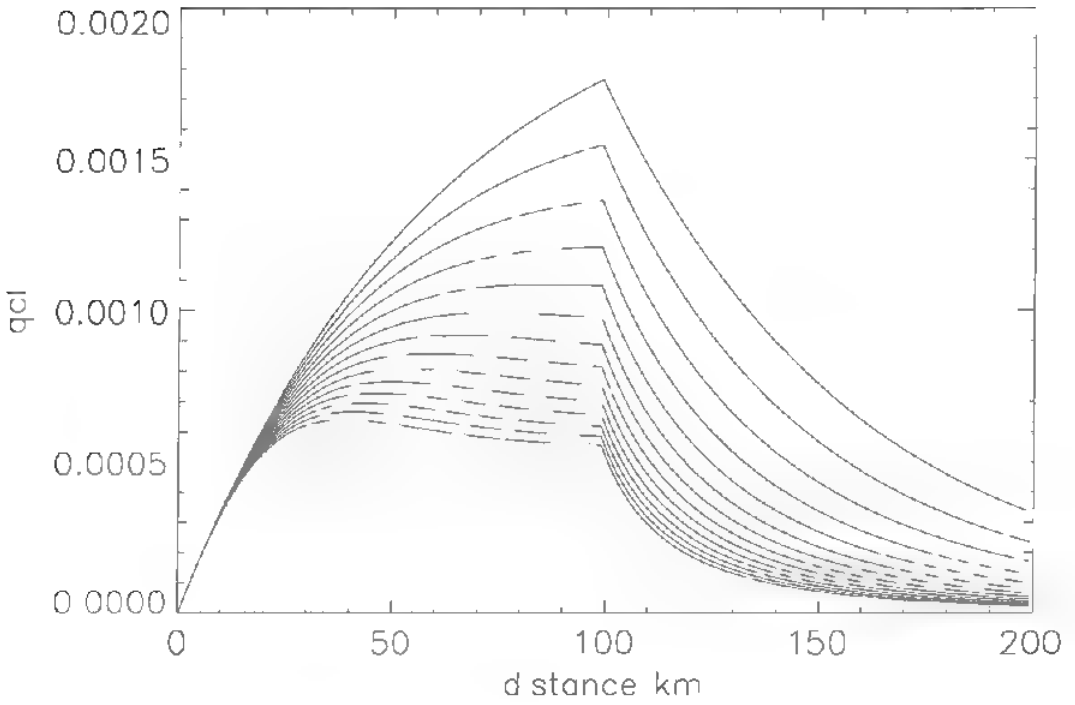

Figure 2(a). Cloud water values from simple model for an upslope followed by a plateau. The top curve represents values on the top level and going down represent successive levels in the model. The gradient, α, is set to 0.02 up to 100km and zero from 100km to 200km.

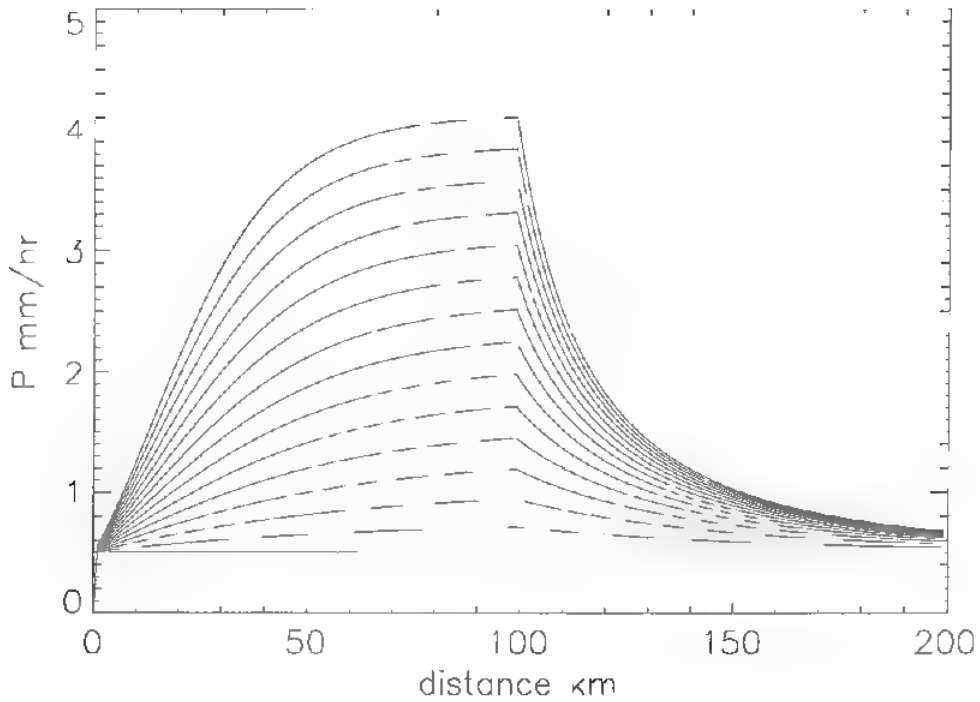

Figure 2(b). As figure 2(a) but for rainrate values. Lowest curve represents top of model and top curve is surface rainrate.

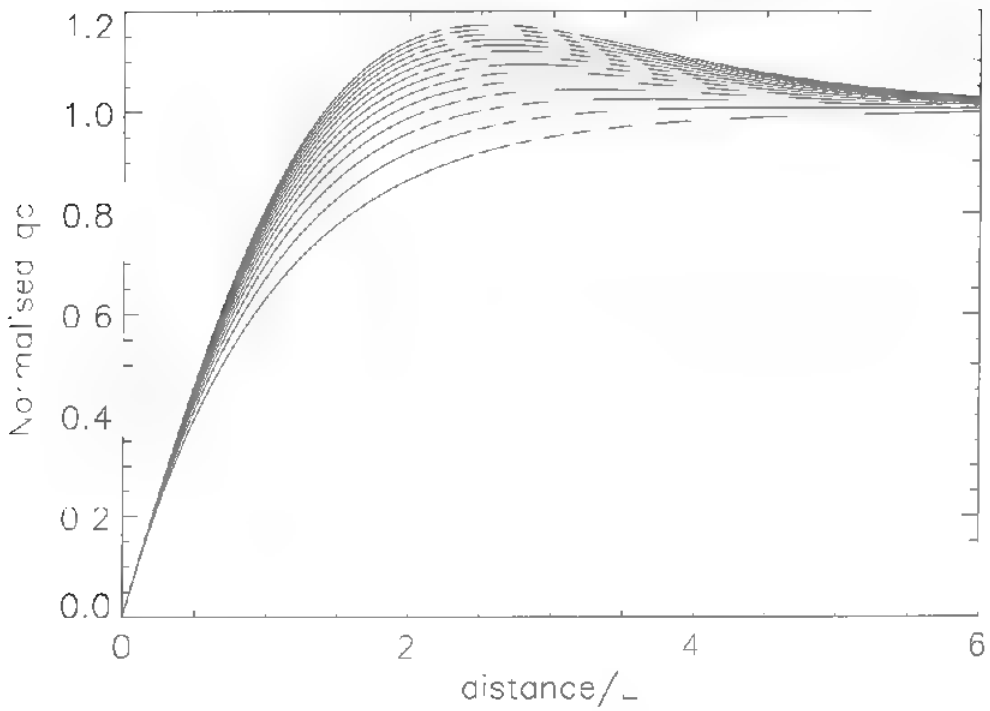

Figure 3(a). Curves for q for an infinite slope with q normalised by q_∞ and distance normalised by L(z). The lowest curve in this figure represents the top of the model.

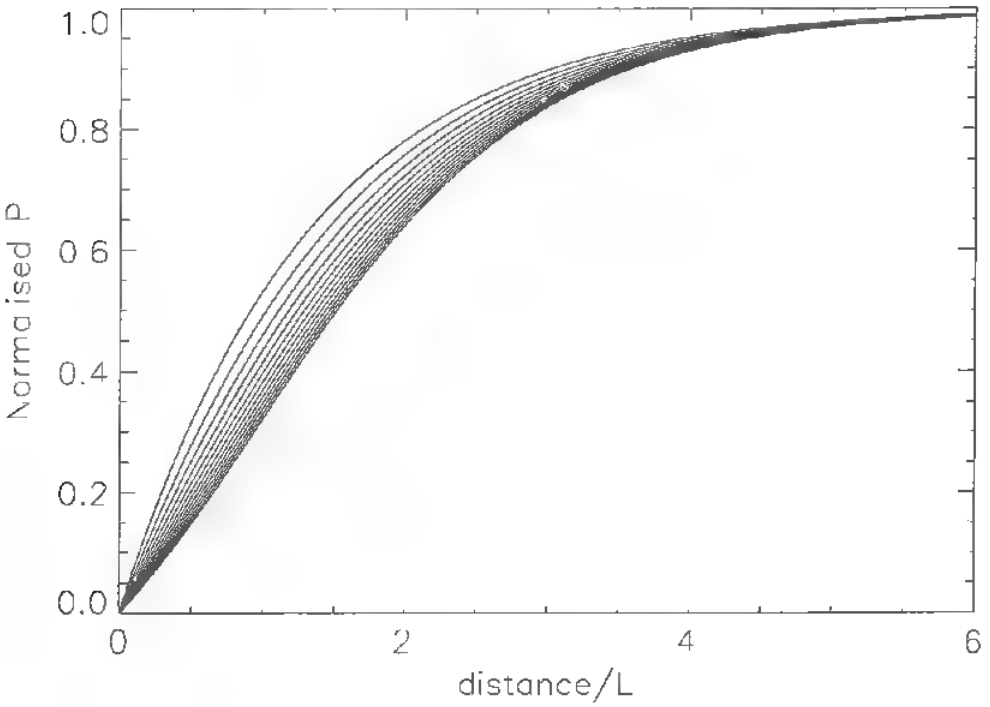

Figure 3(b) Rainrate value curves normalised as described in text with distance normalised as above. The lowest curve in this figure represents the surface rainrate.

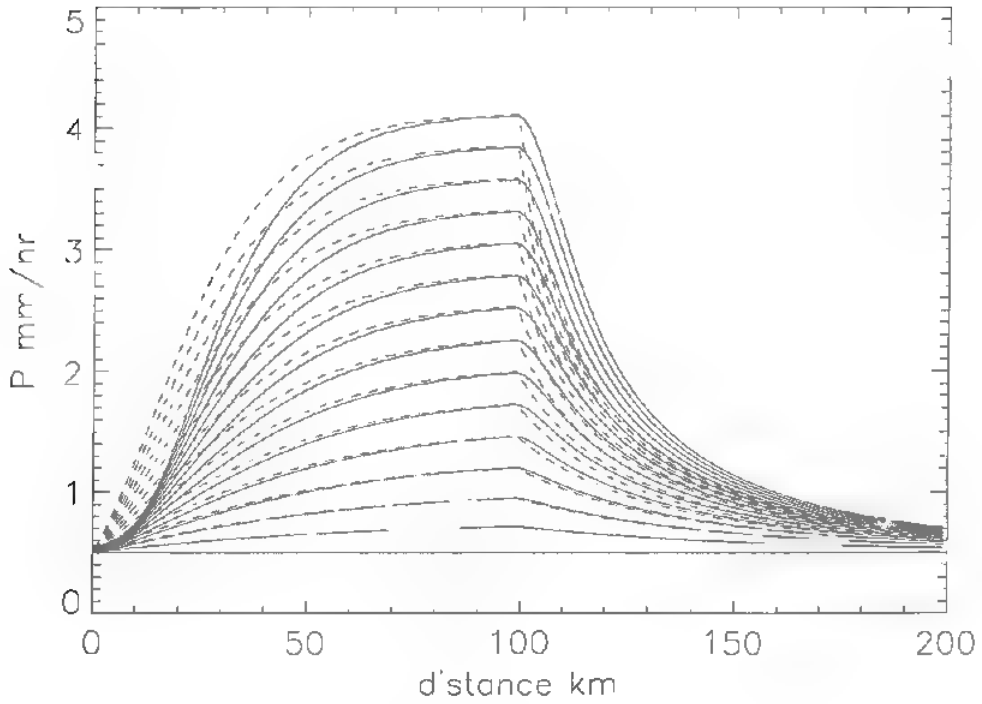

Figure 3(c) Rainfall rate curves from simple model for 100km upslope followed by plateau (as for figure 2). Solid lines show calculation including drift of rain. Dotted are without (as fig 2(b)) for comparison.

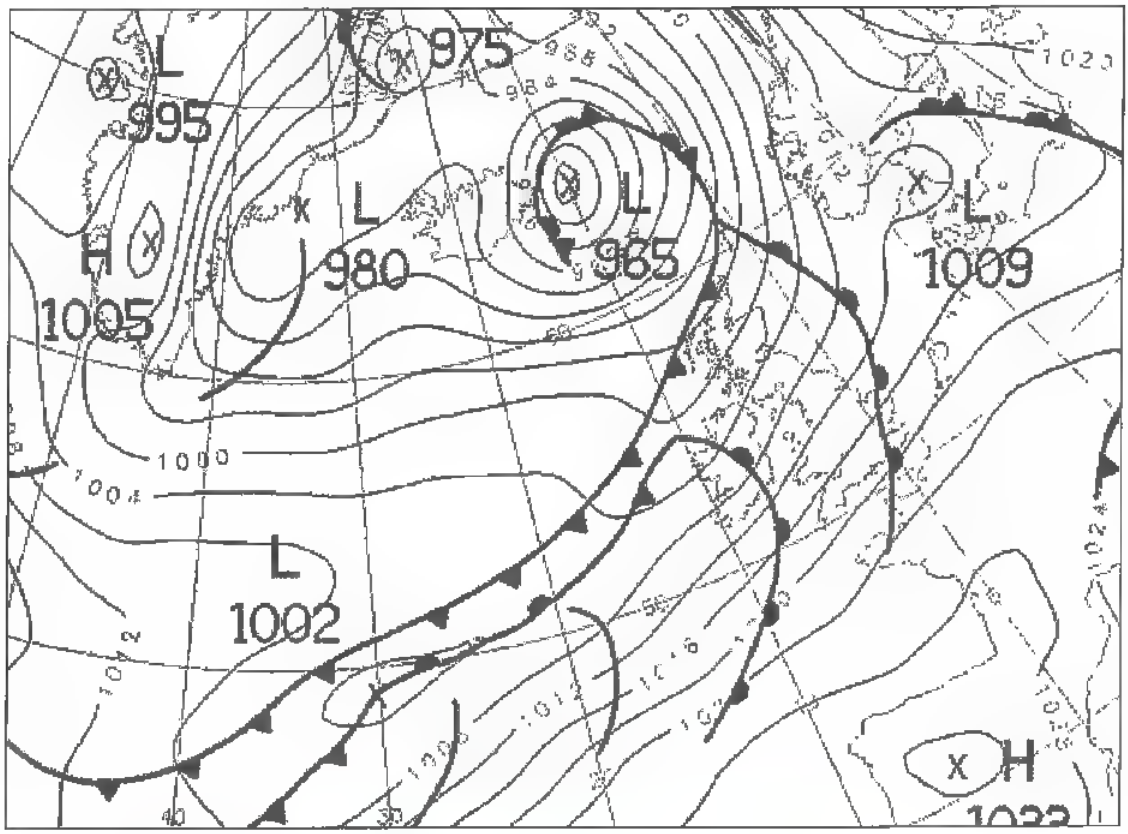

Figure 4. Met Office Analysis chart for 0Z 29 Nov 2001

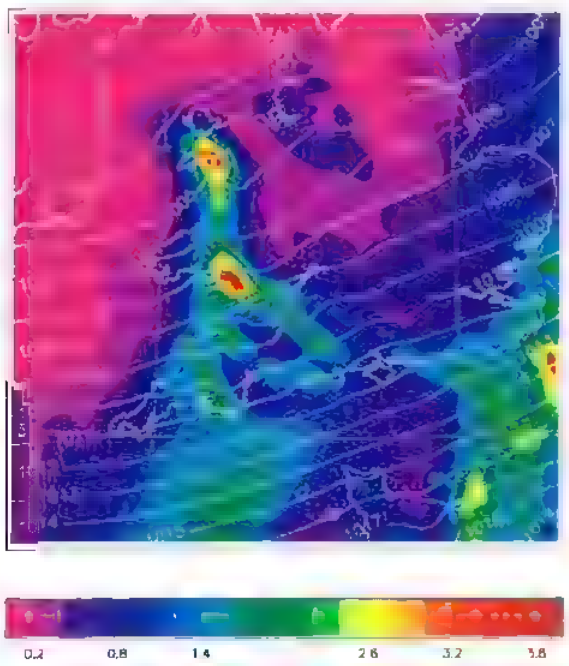

Figure 5. 12Z Large scale rainrate and mean sea level pressure from UM version 5.2 12km run started at 1Z.

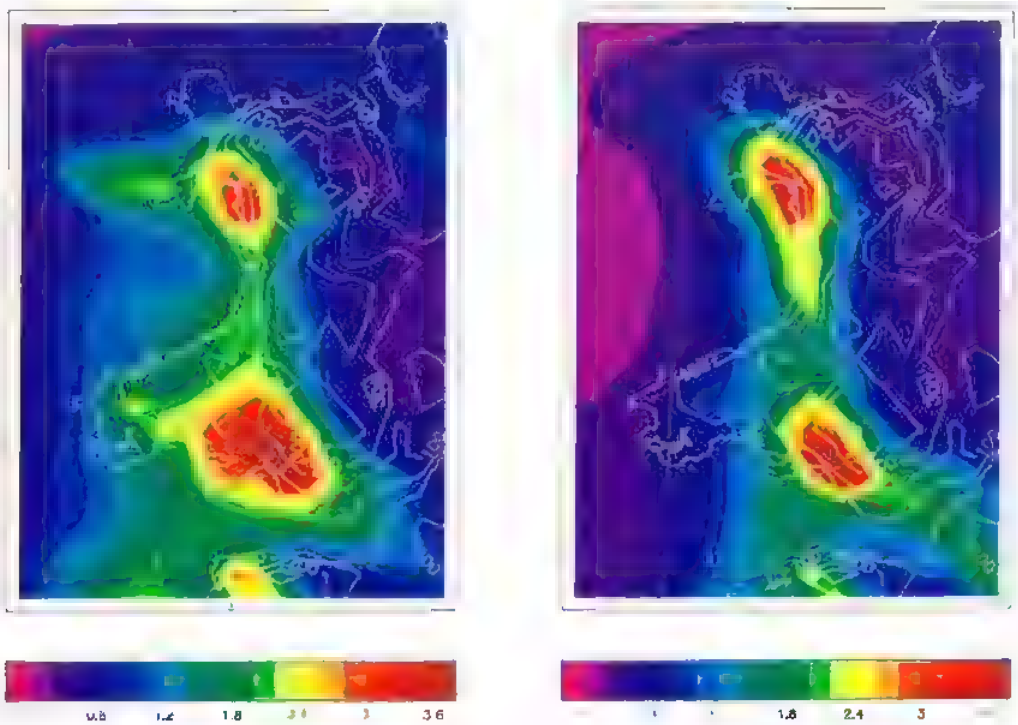

Figure 6. Large scale rainrate at 11 (left) and 12Z with orography from 12km model. The line across the S Wales patch of rain shows the positions of the cross section in following figures.

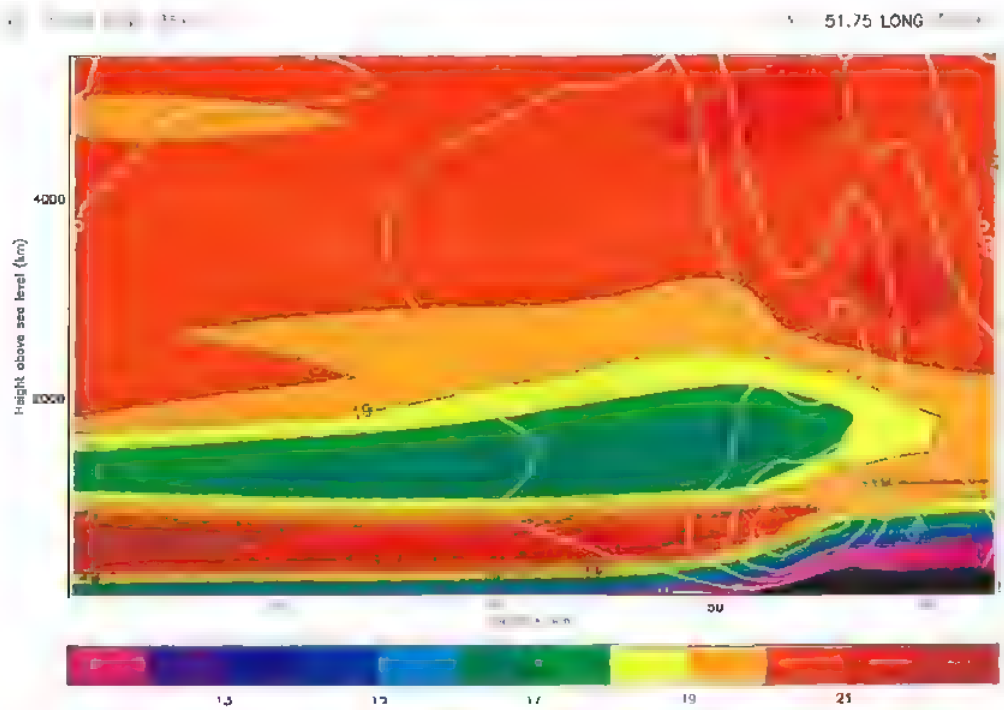

Figure 7. Cross section of along section wind (colours) and vertical velocity (white contours) along line in Figure 6 at 12Z.

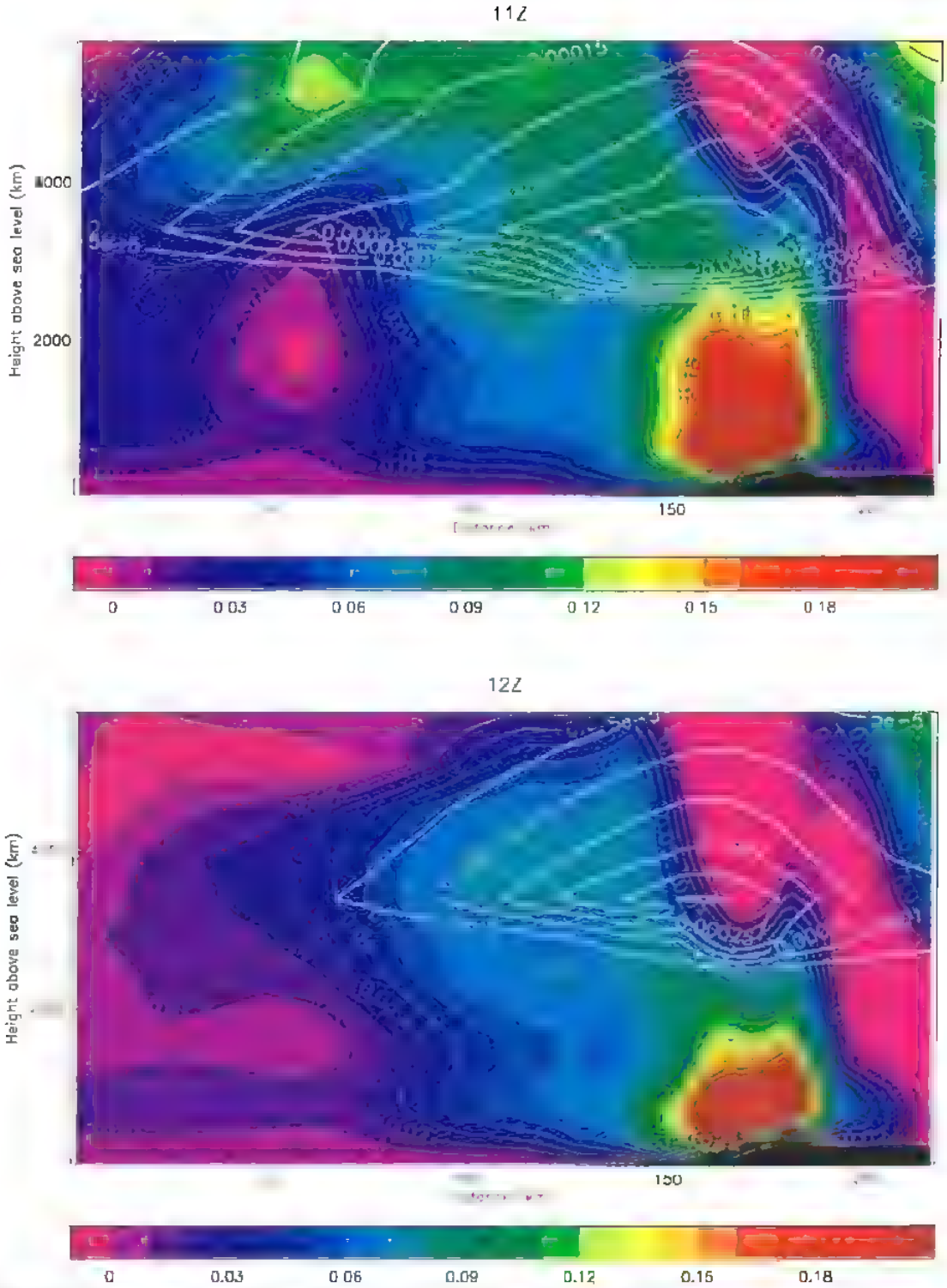

Figure 8 Cross sections of vertical velocity (colours) and qef (contours) at 11 and 12Z. The cross sections are twice as long as figure 7 (extended SW) and have a different vertical scale.

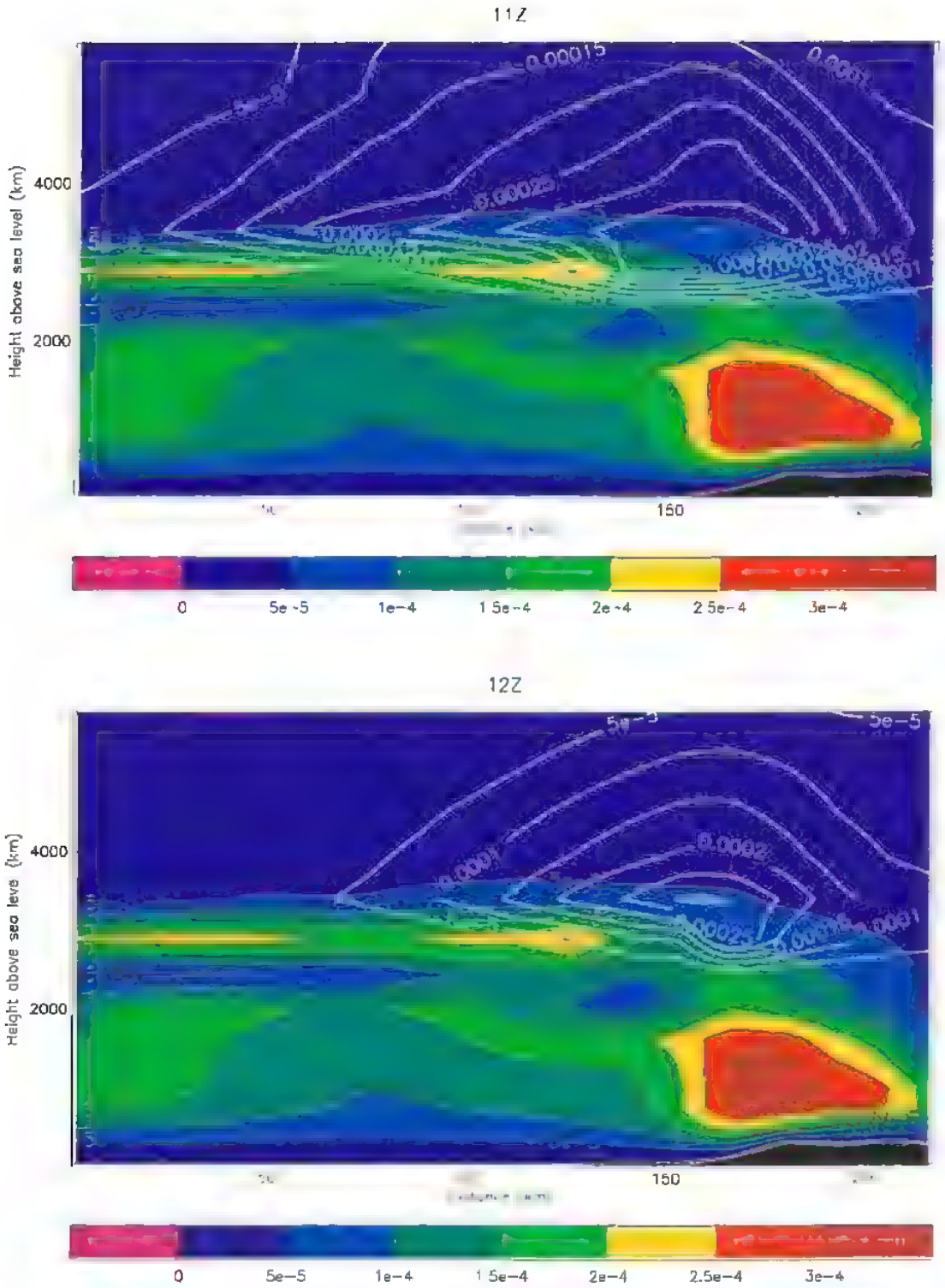

Figure 9. Cross sections as for figure 8 but of qcl (colours) and qcf (contours)

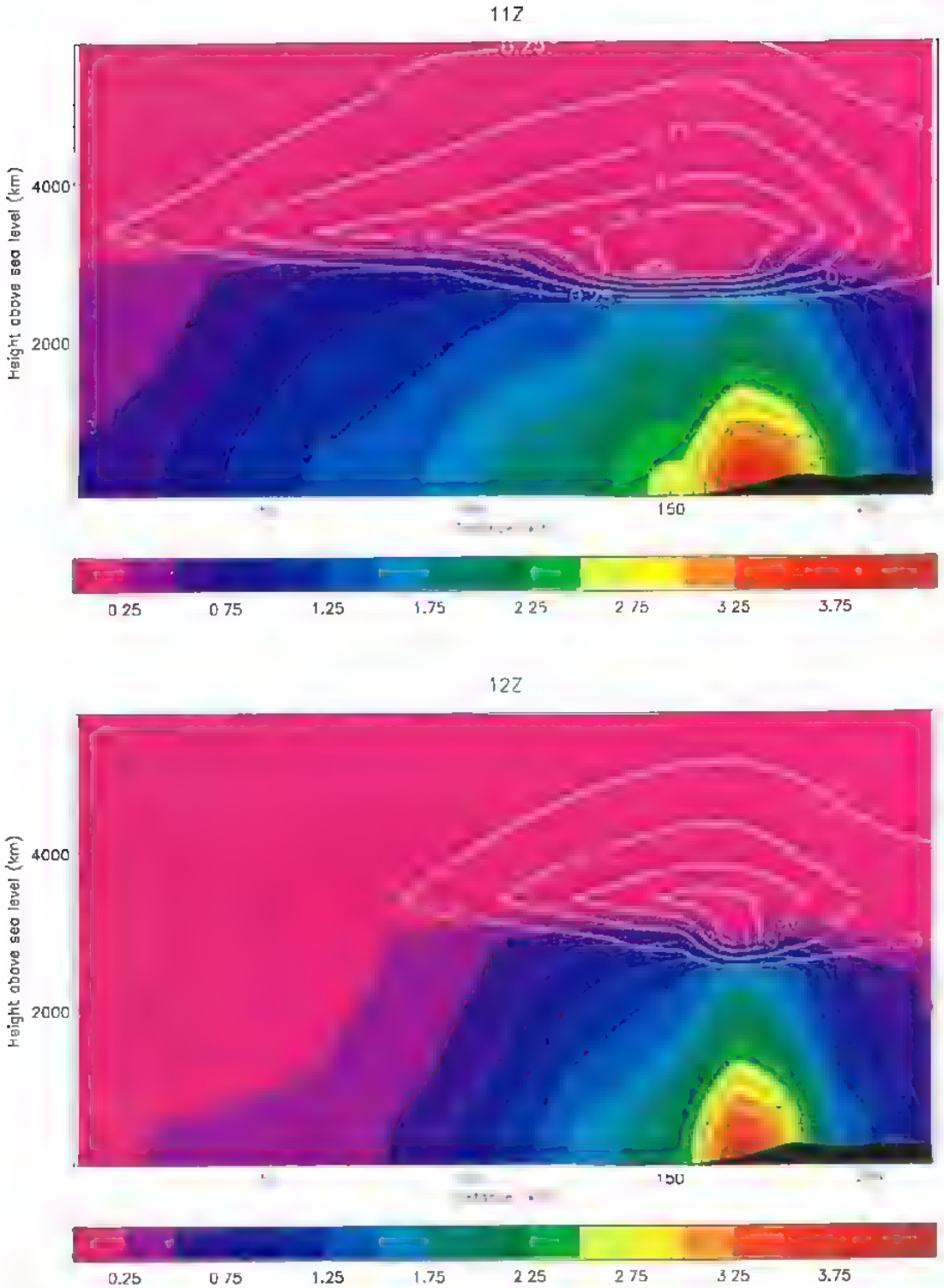

Figure 10. As figure 8 but rainfall rate (colours) and snowfall rate (contours) both in mm/hr.

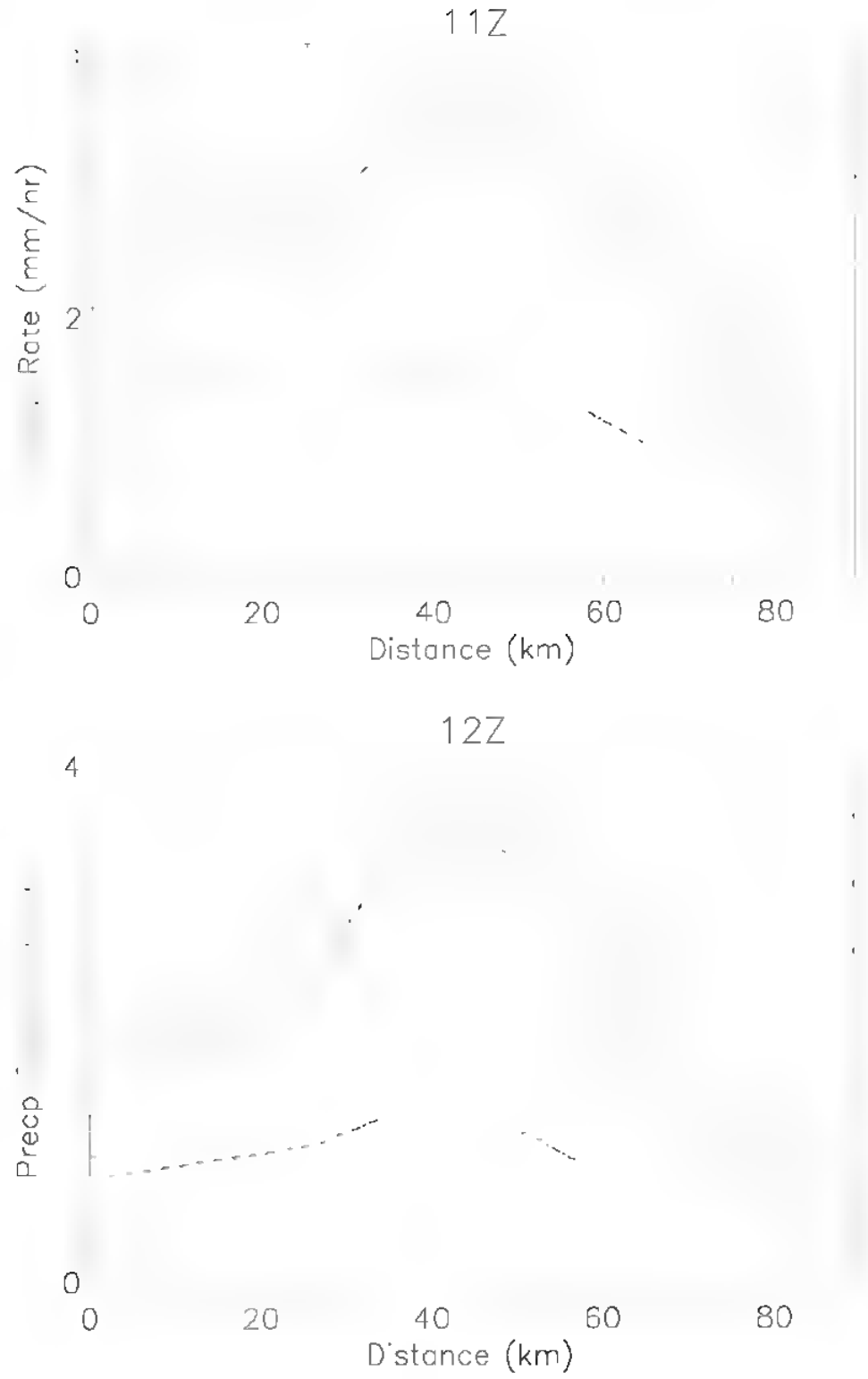

Figure 11 Comparisons of rainfall rates from UM version 5.2 12km runs with the simple seeder-feeder model along the same cross section as shown in figure 7. The solid line in each case is seeder feeder model surface rain rate and the top dotted line is the UM surface rain rate. The lower dotted line is imposed precip rate at top of seeder-feeder model taken from UM run

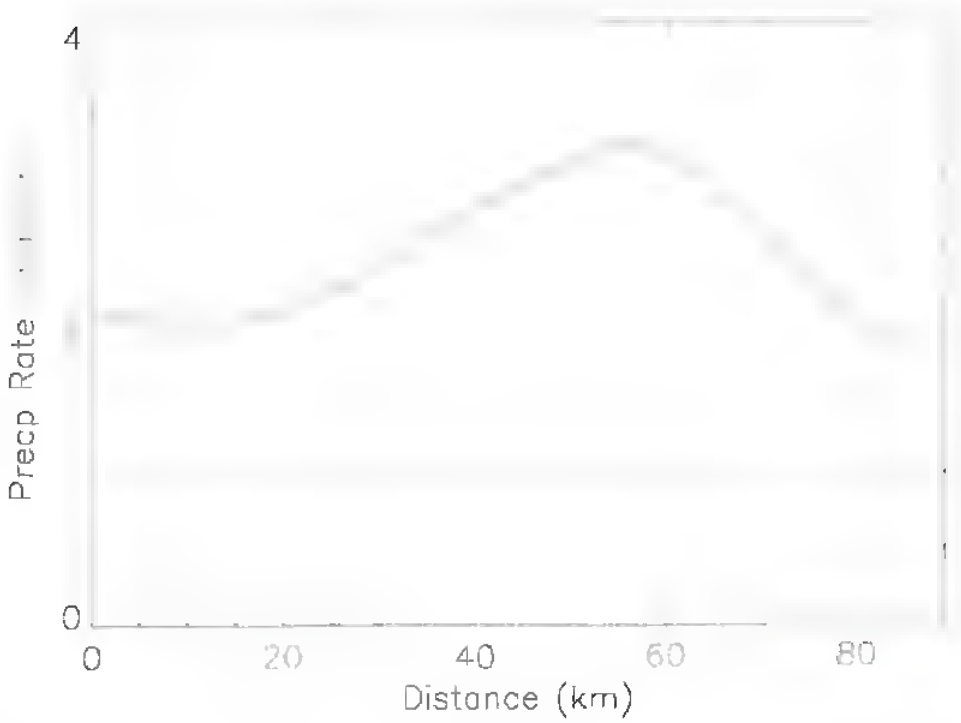

Figure 12. Results from seeder feeder model for same vertical velocity and other parameters as in figure 11 but with constant precipitation rate assumed at the top. Top (solid) line is surface rainfall rate and lower is rainfall rate at the top.

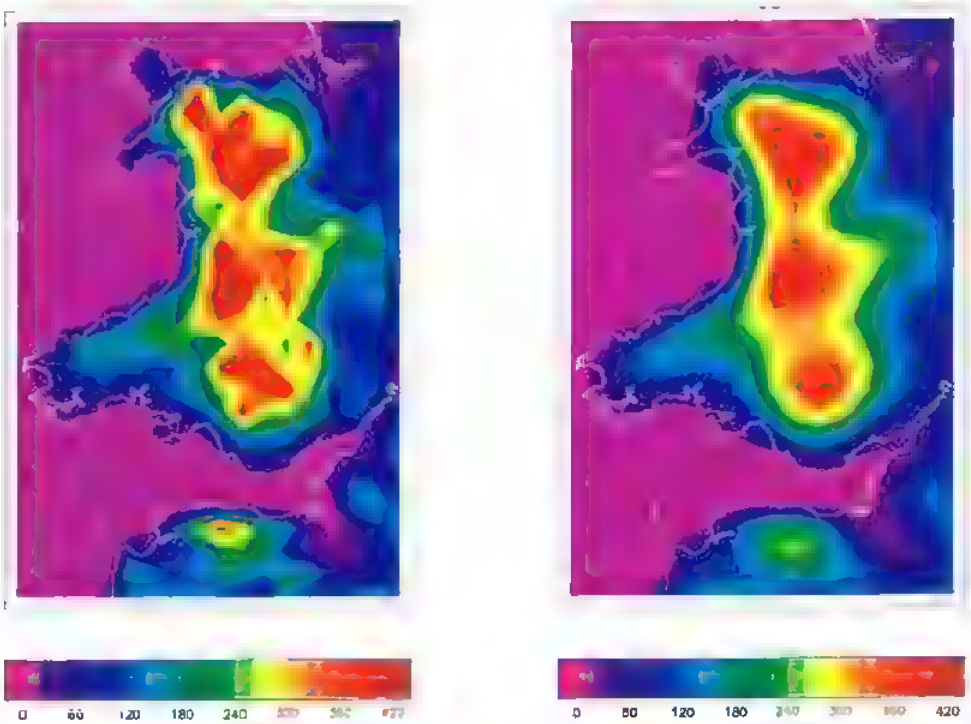

Figure 13. Comparison of vn 4.5 UK mesoscale 12km orography (left) with smoothed orography to be used with vn 5.2. Note that the coastline shown is for location purposes only and is more detailed than that used in the 12km model.

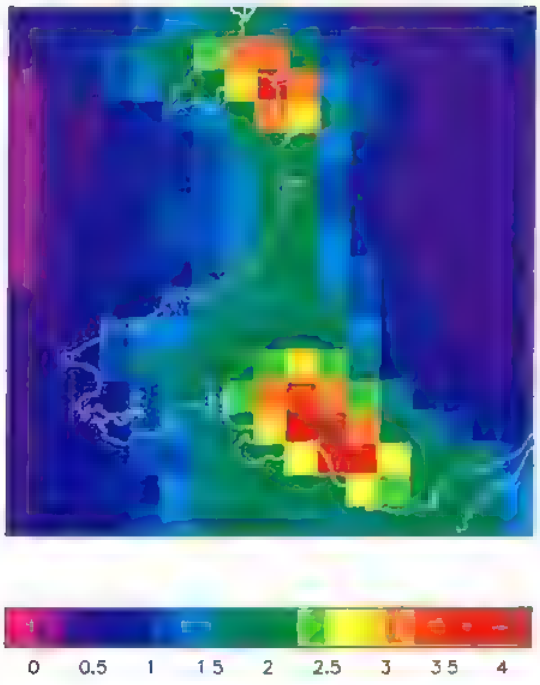

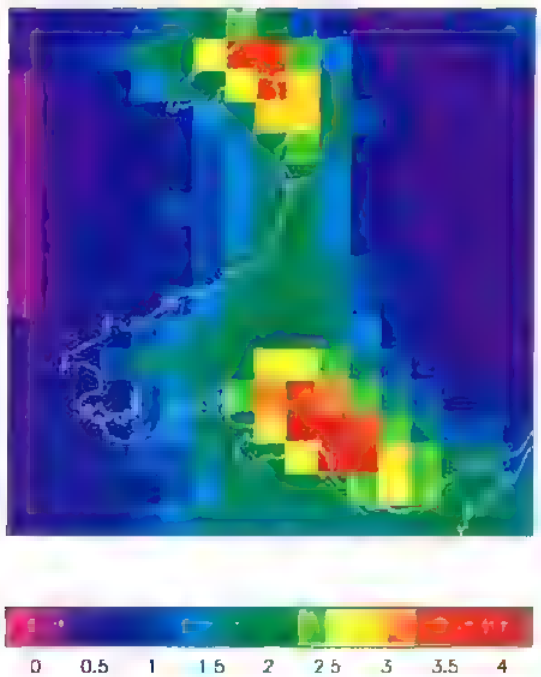

Figure 14. 11-12Z accumulated rainfall from 12km models with vn4.5 orography (top) and the vn5.2 smoothed orography (bottom).

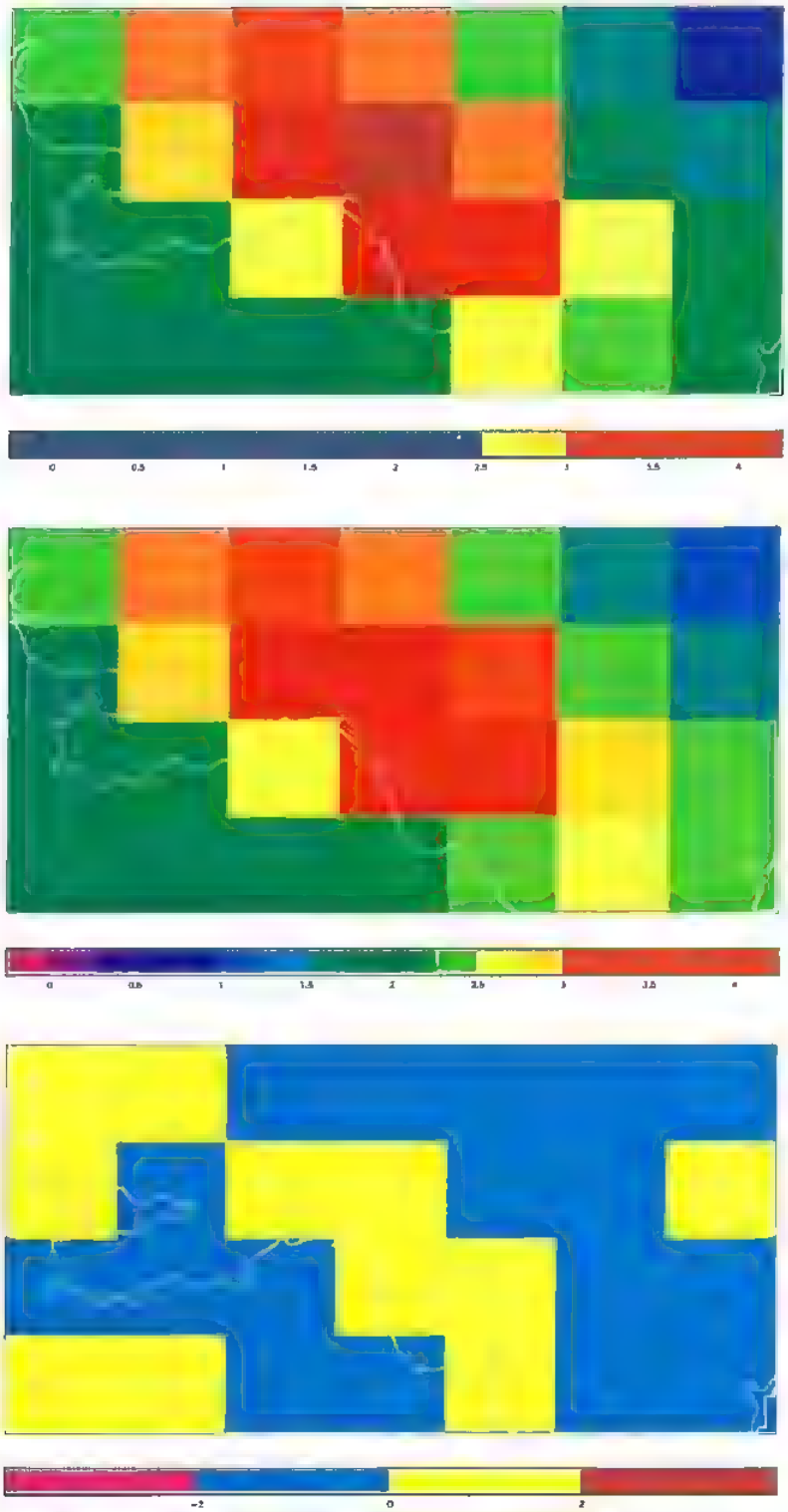

Figure 15 Top two frames show 11-12Z accumulated rainfall from 12km models over area of interest in S Wales. Top: run with vn4.5 unsmoothed orography Middle: run with smoothed vn5.2 orography. Bottom frame shows sign of difference with yellow colour meaning that unsmoothed orography run has higher rainfall in that gridbox.

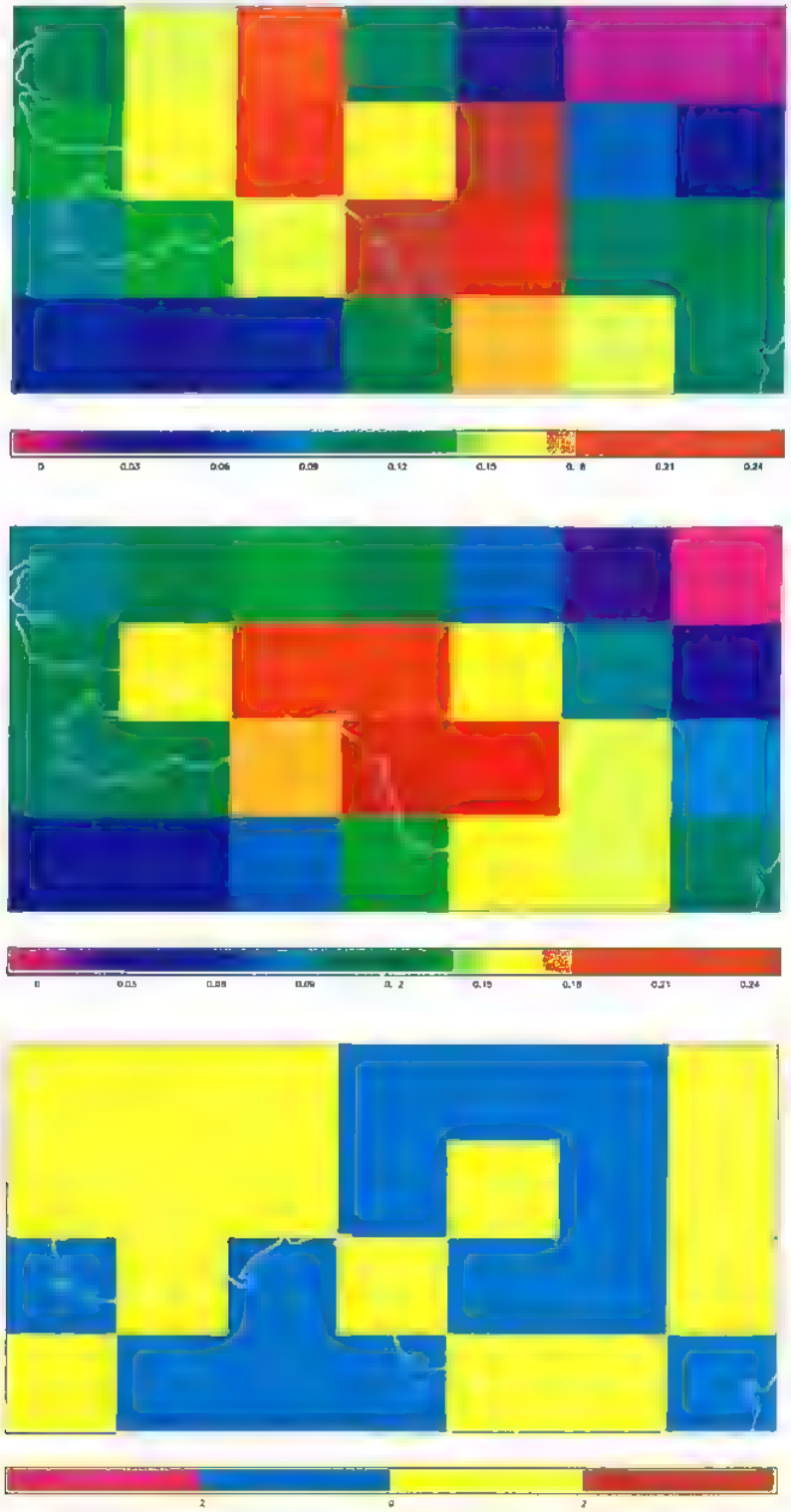

Figure 16. As for figure 15 but with 12Z vertical velocity at 500m fields.

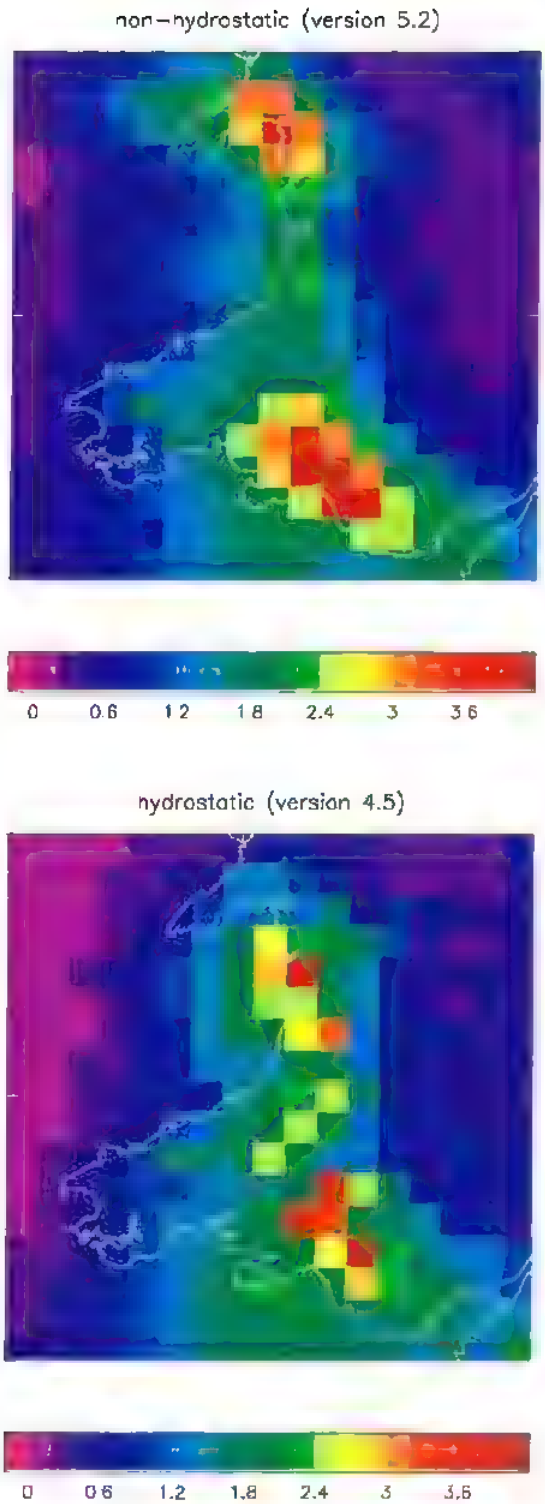

Figure 17. 11-12Z accumulated rainfall from 12km models. Top: non-hydrostatic model (version 5.2) Bottom: hydrostatic model (version 4.5).

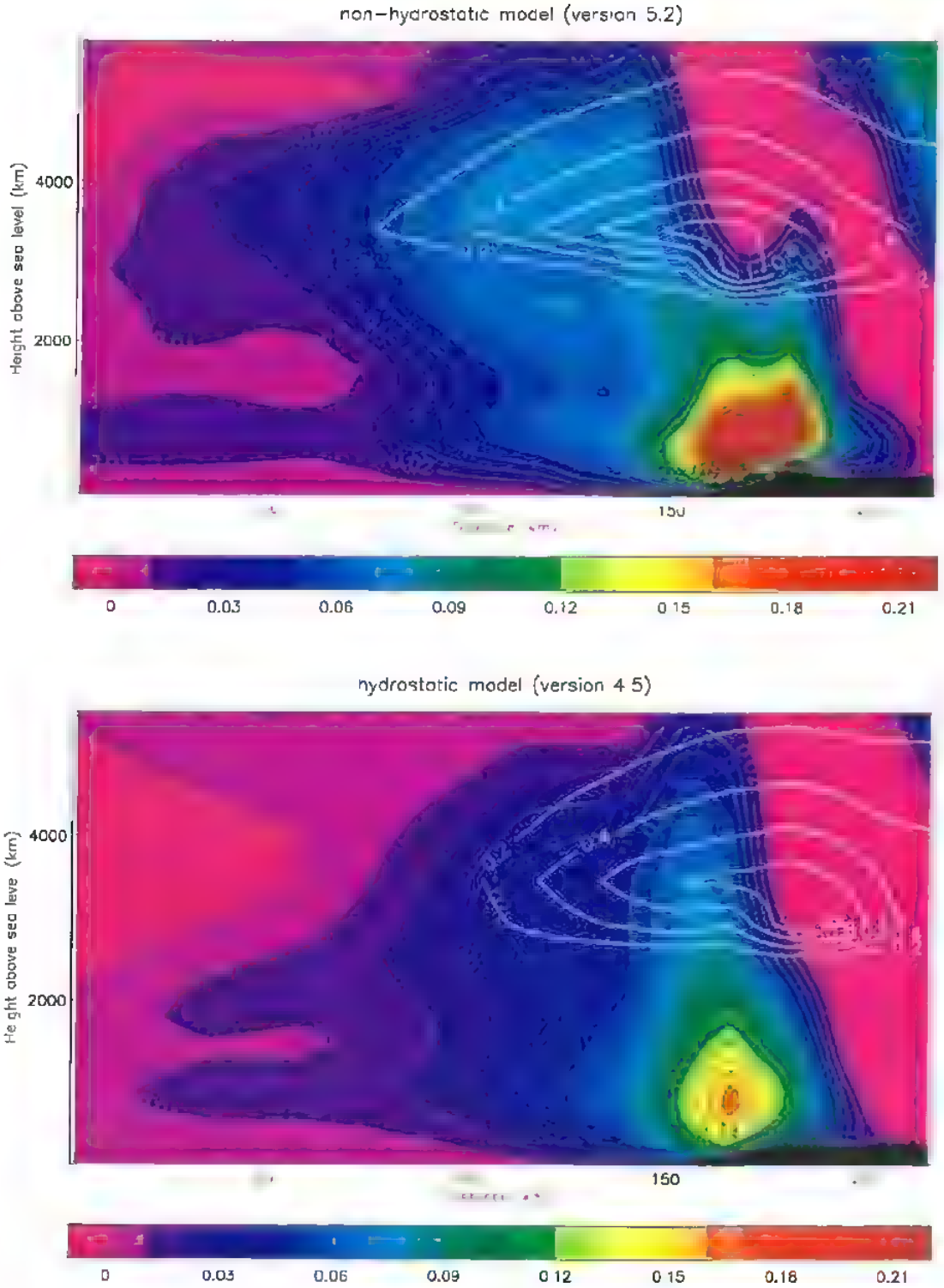

Figure 18. Cross section along same line as figure 8 showing vertical velocity (colours) and snowfall rate (white contours) at 12Z for non-hydrostatic (top) and hydrostatic models.

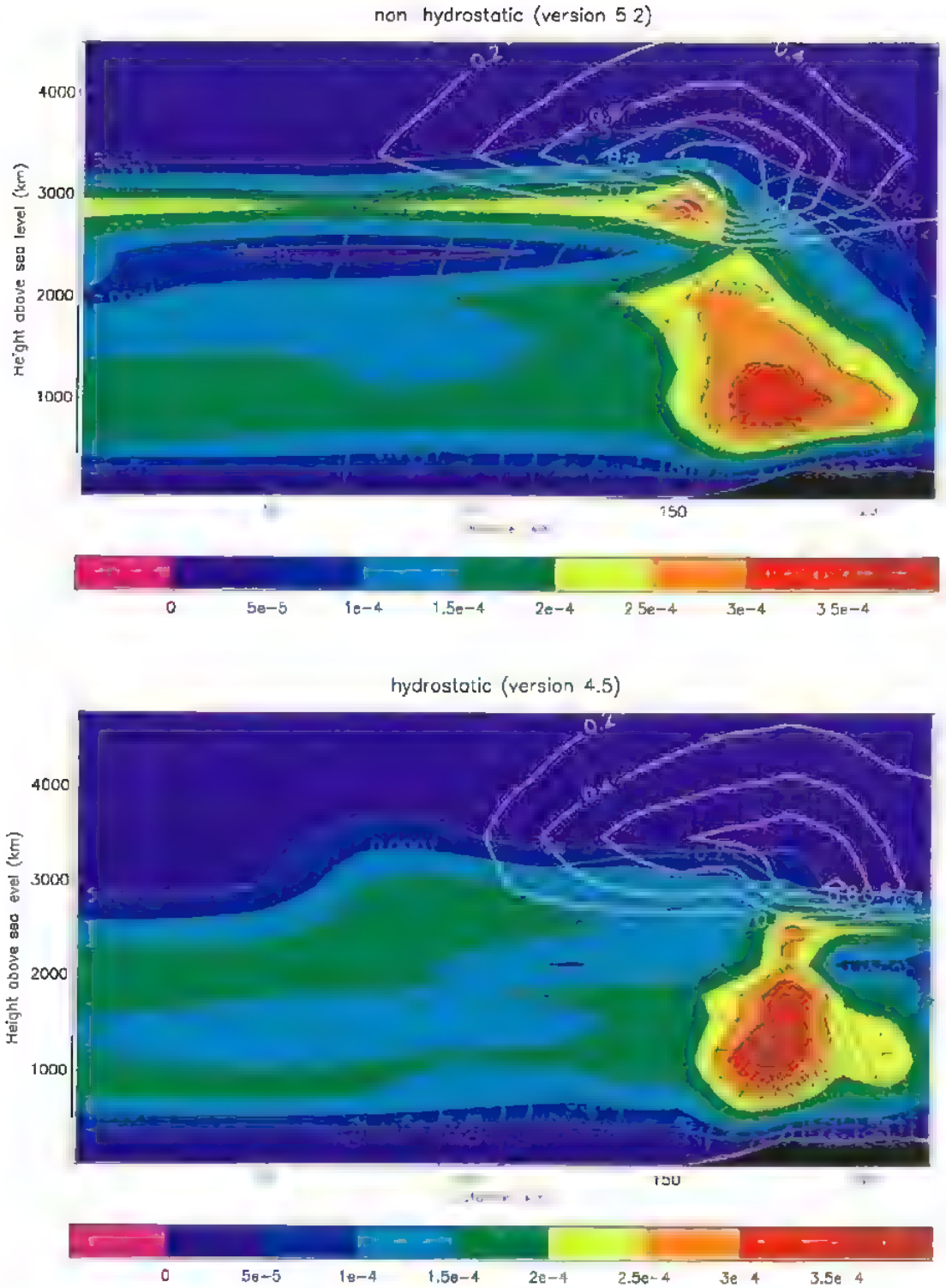

Figure 19. As figure 18 showing cloud water (colours), snowfall rate (white contours) and rainfall rate (black contours)

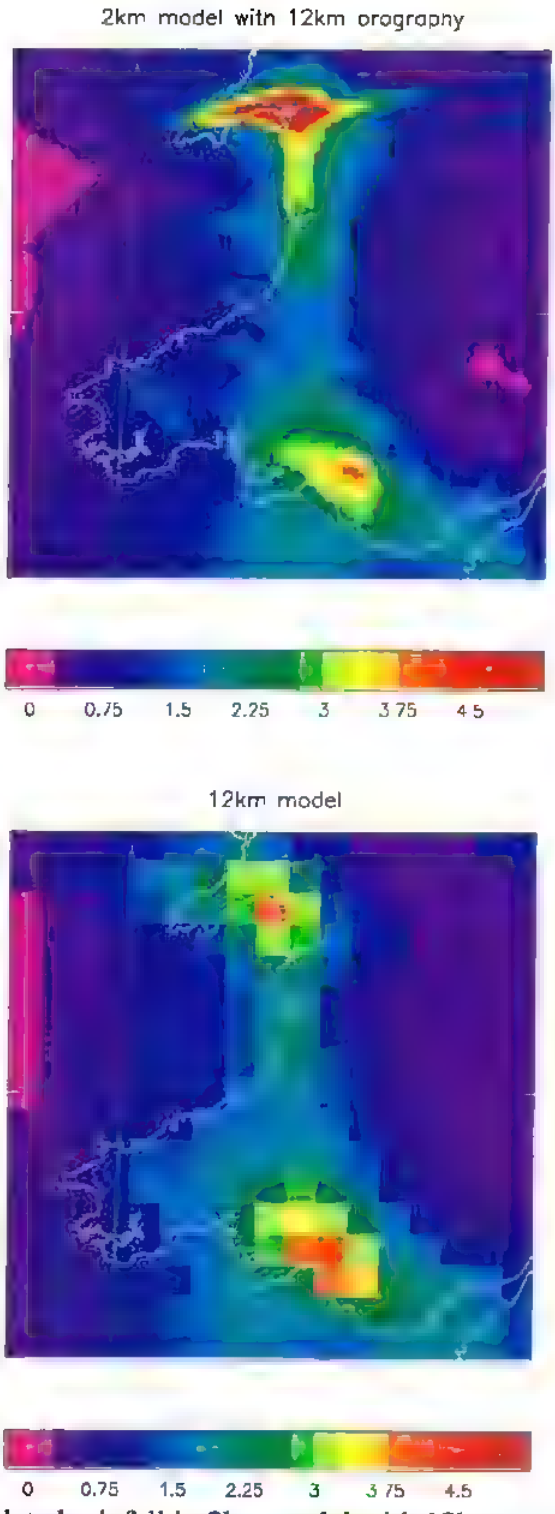

Figure 20. 11-12Z accumulated rainfall in 2km model with 12km orography (top) and in 12km model.

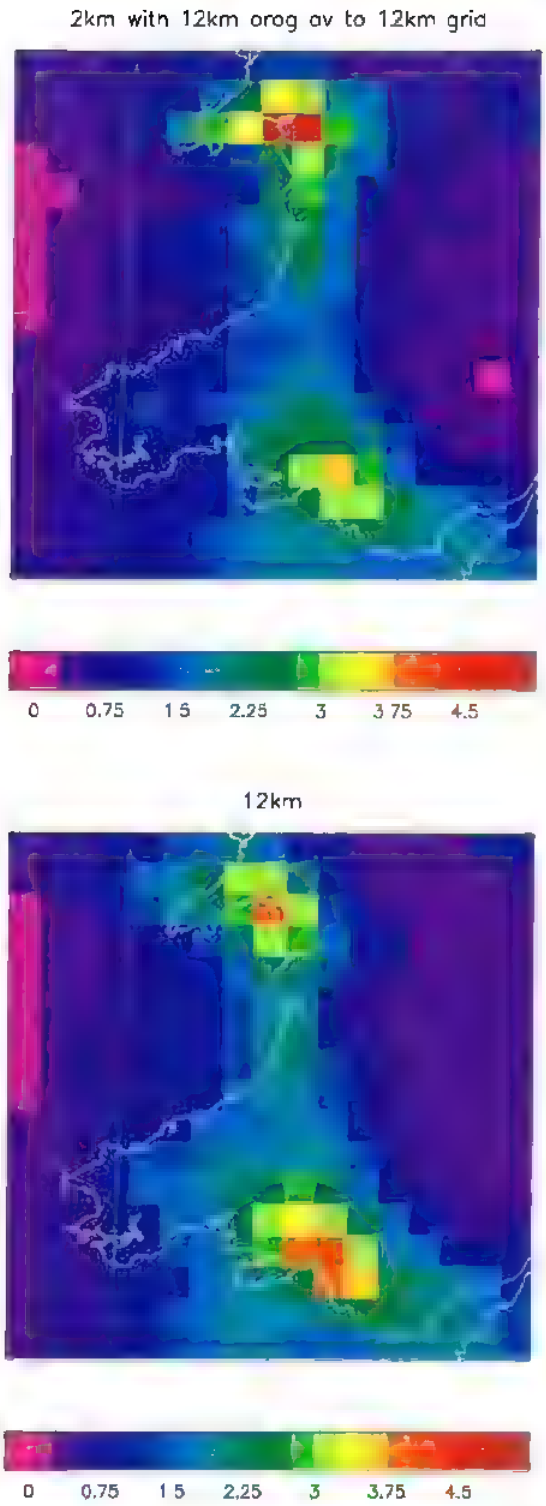

Figure 21. As figure 20 except 2km model data has been area averaged to 12km model grid to enable direct comparison of average values.

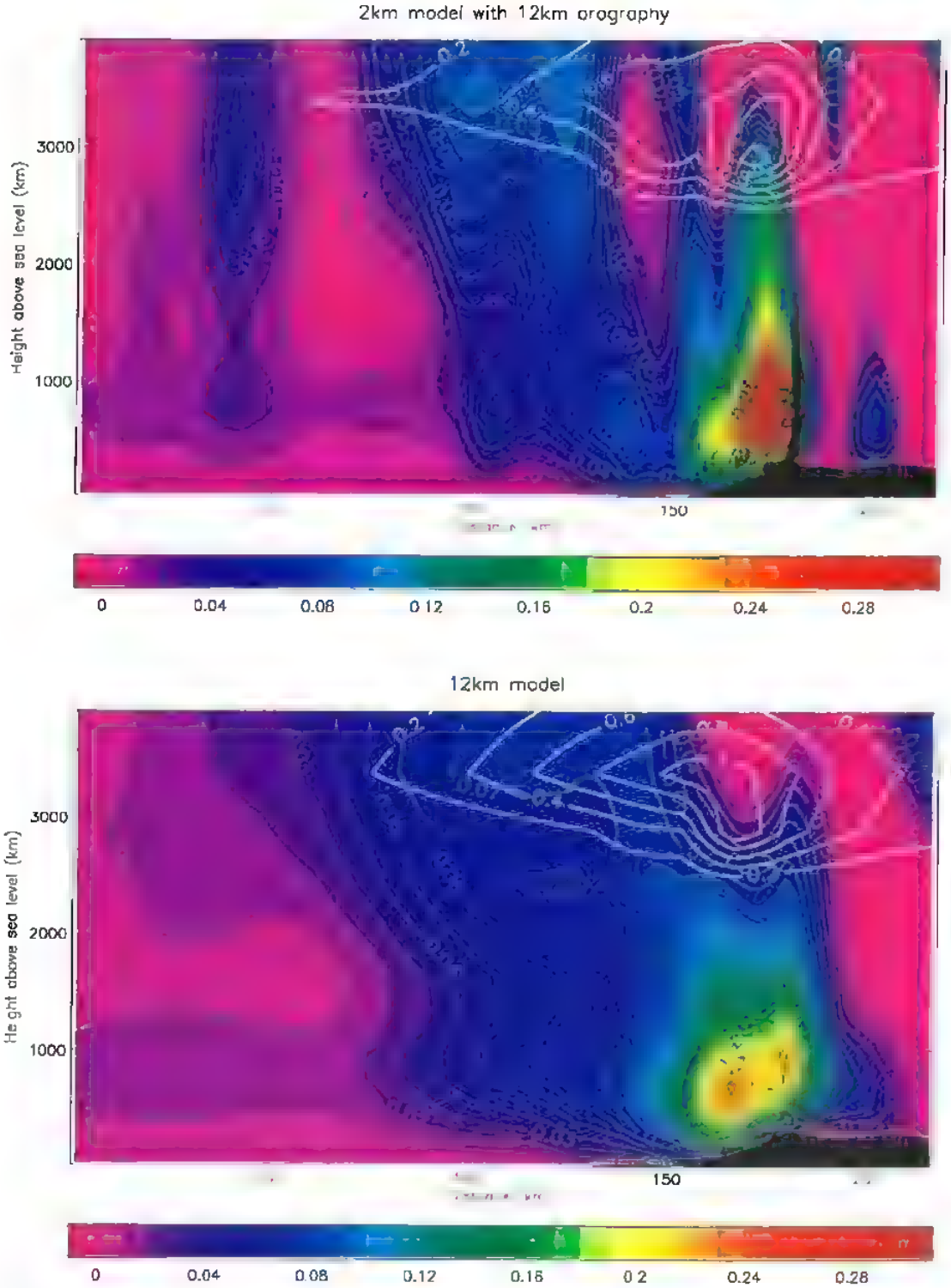

Figure 22. Cross sections along same cross section as figure 8 showing vertical velocity (colours) and snowfall rate (white contours) in the 2km model with 12km orography and the 12km model.

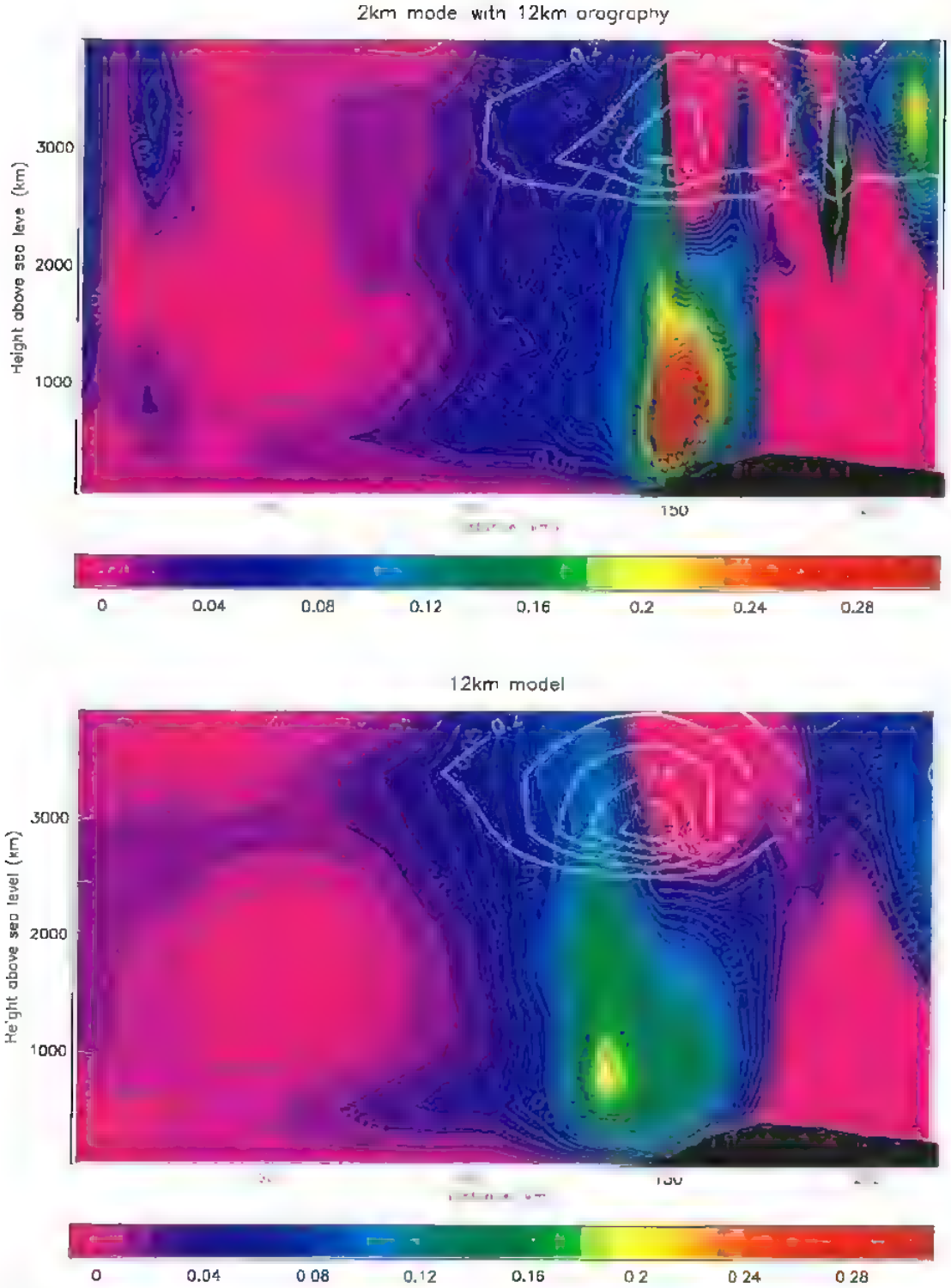

Figure 23. As fig 22 except for cross section (shown in figure 20) cutting across Snowdonia.

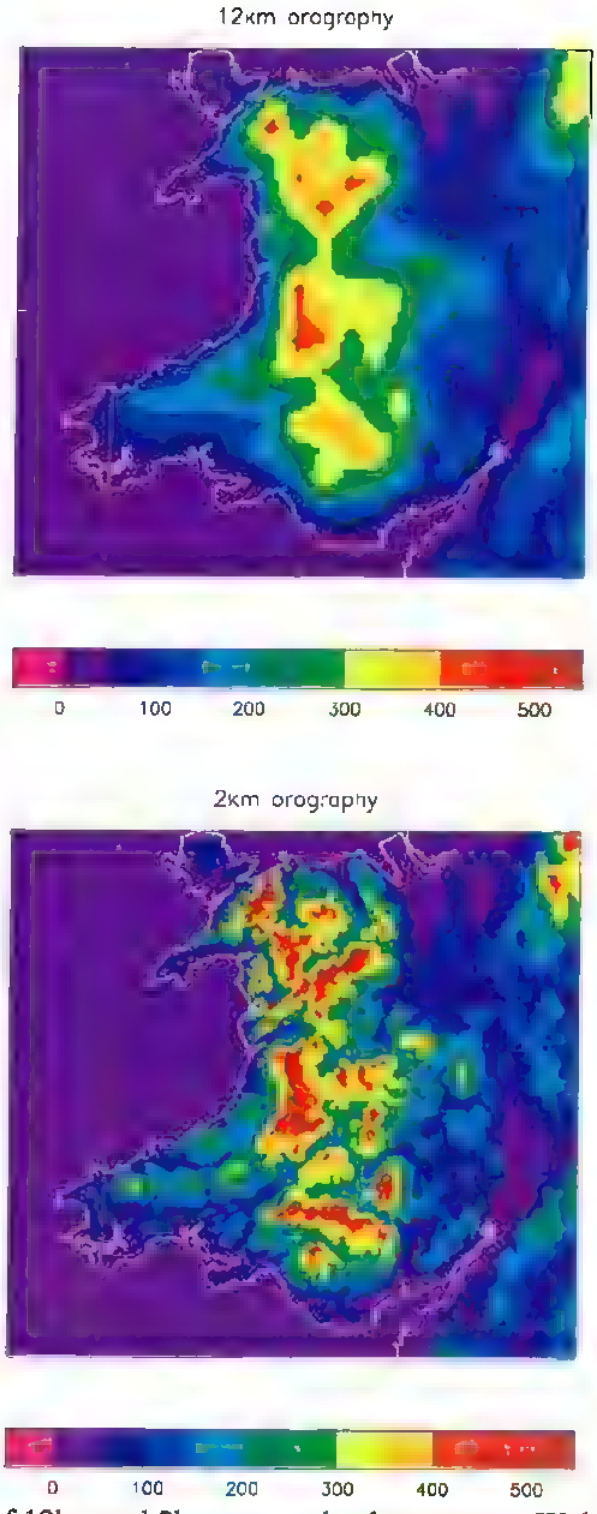

Figure 24. Comparison of 12km and 2km orography datasets over Wales.

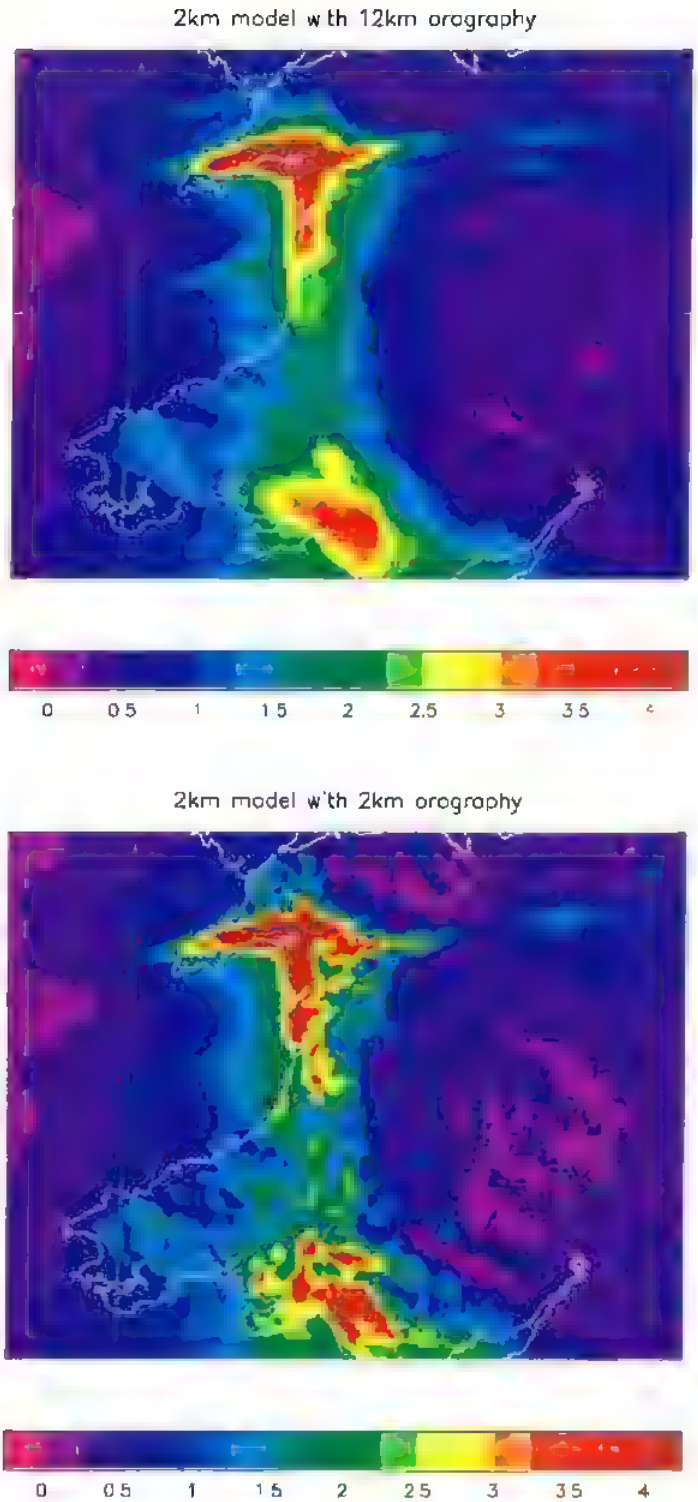

Figure 25. 11-12Z accumulated rainfall in 2km model with 12km orography (top) and 2km model with 2km orography (bottom).

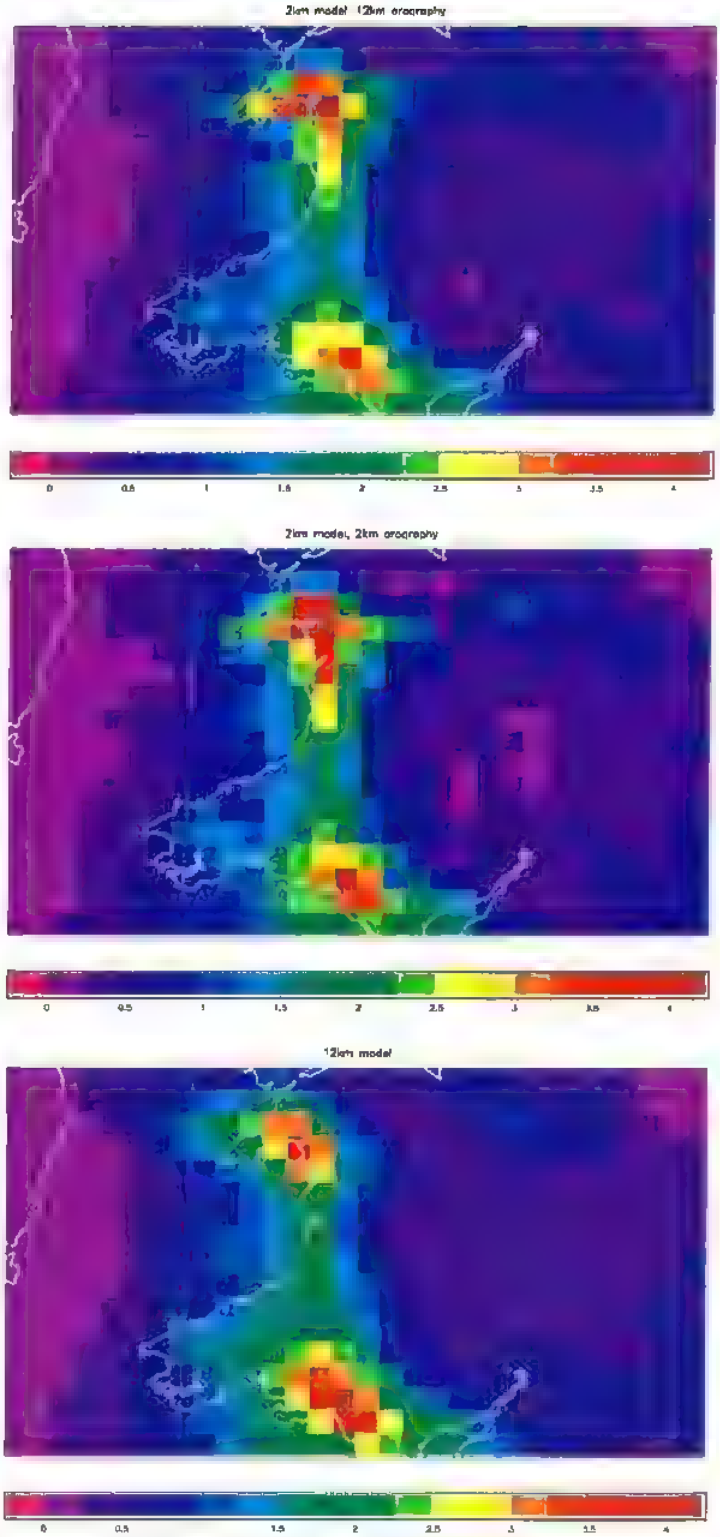

Figure 26 Comparison of 11-12Z accumulated rainfall for 2km model with 12 and 2km orography and 12km model. The 2km model data has been averaged to the 12km grid

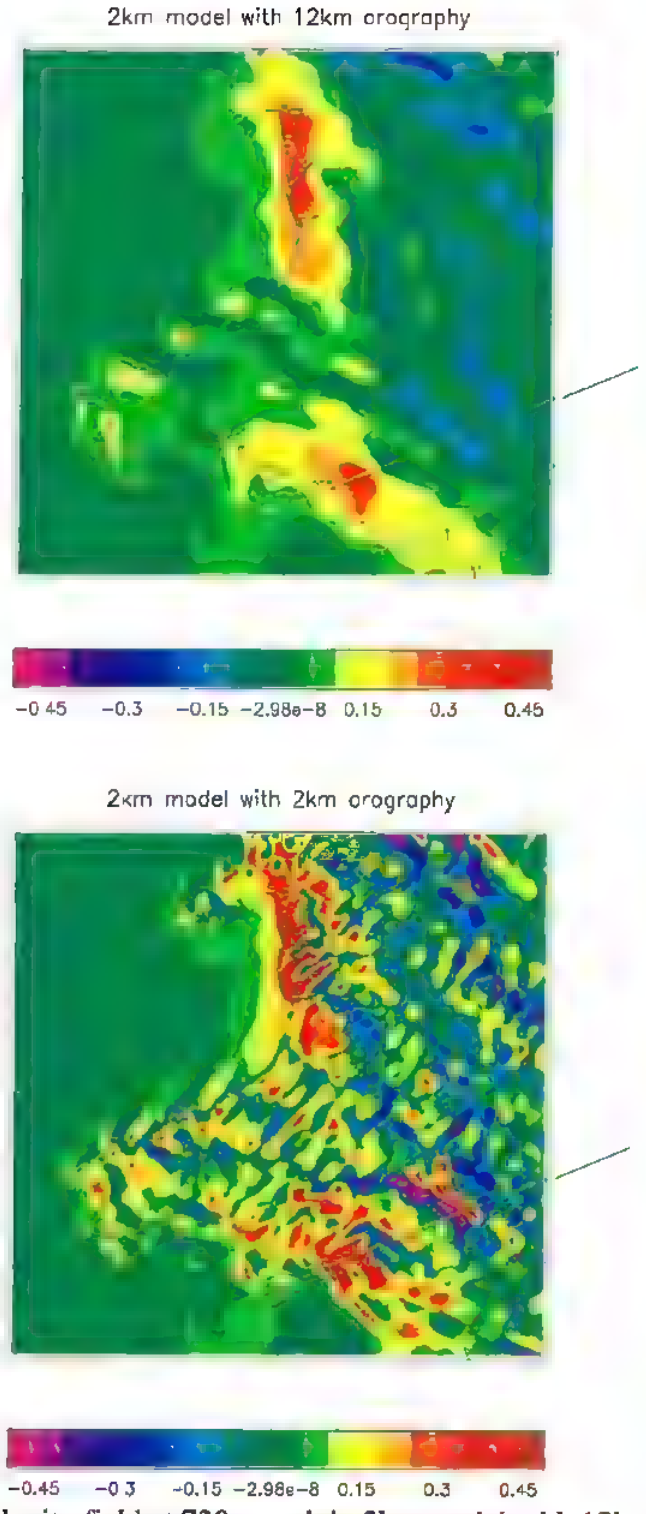

Figure 27 12Z Vertical velocity field at 720m a.s.l. in 2km model with 12km and 2km orography.

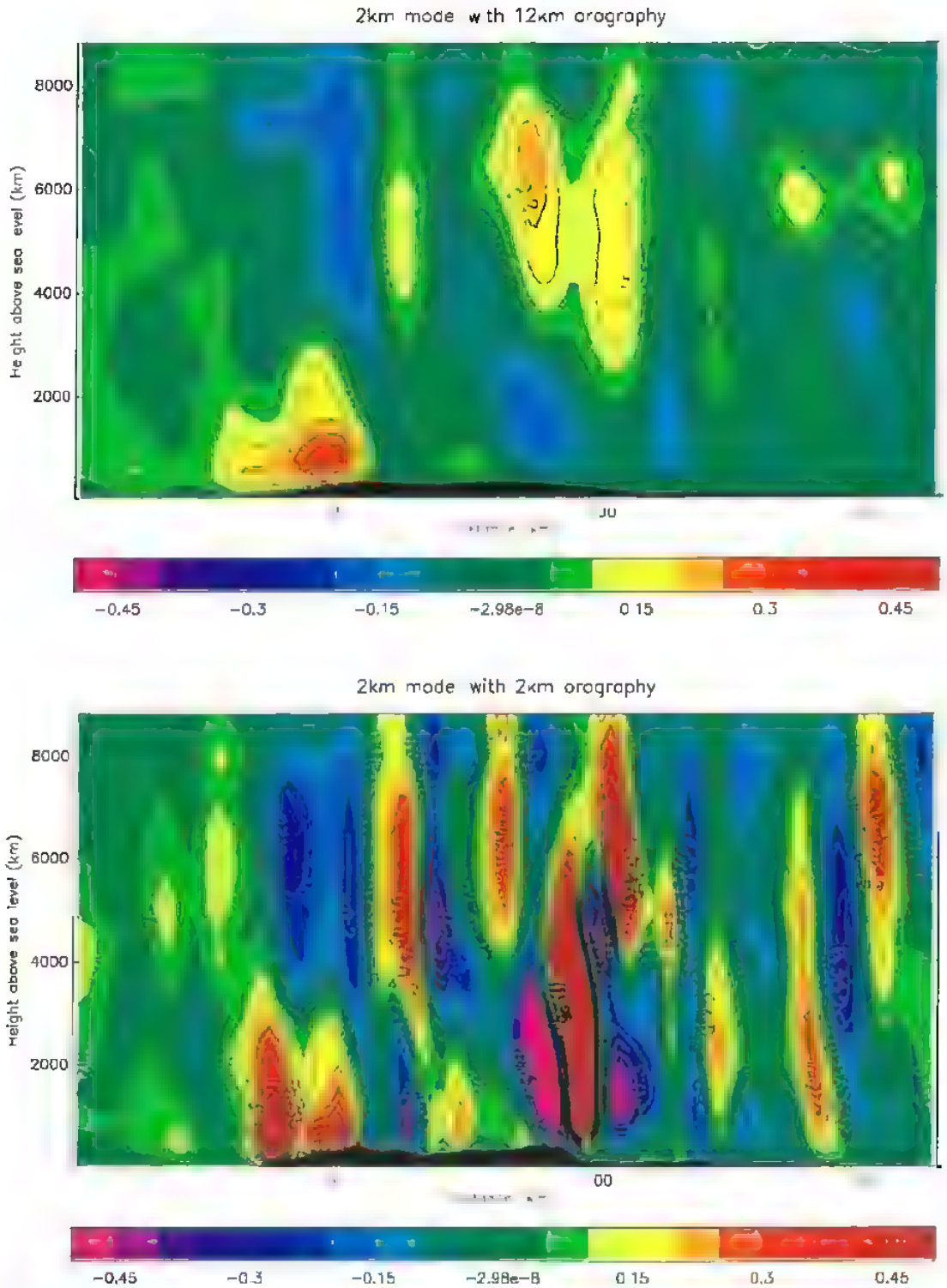

Figure 28. Cross sections along lines in figure 27 of vertical velocity in the same two models. Note the vertical scale is extended compared to previous cross sections.

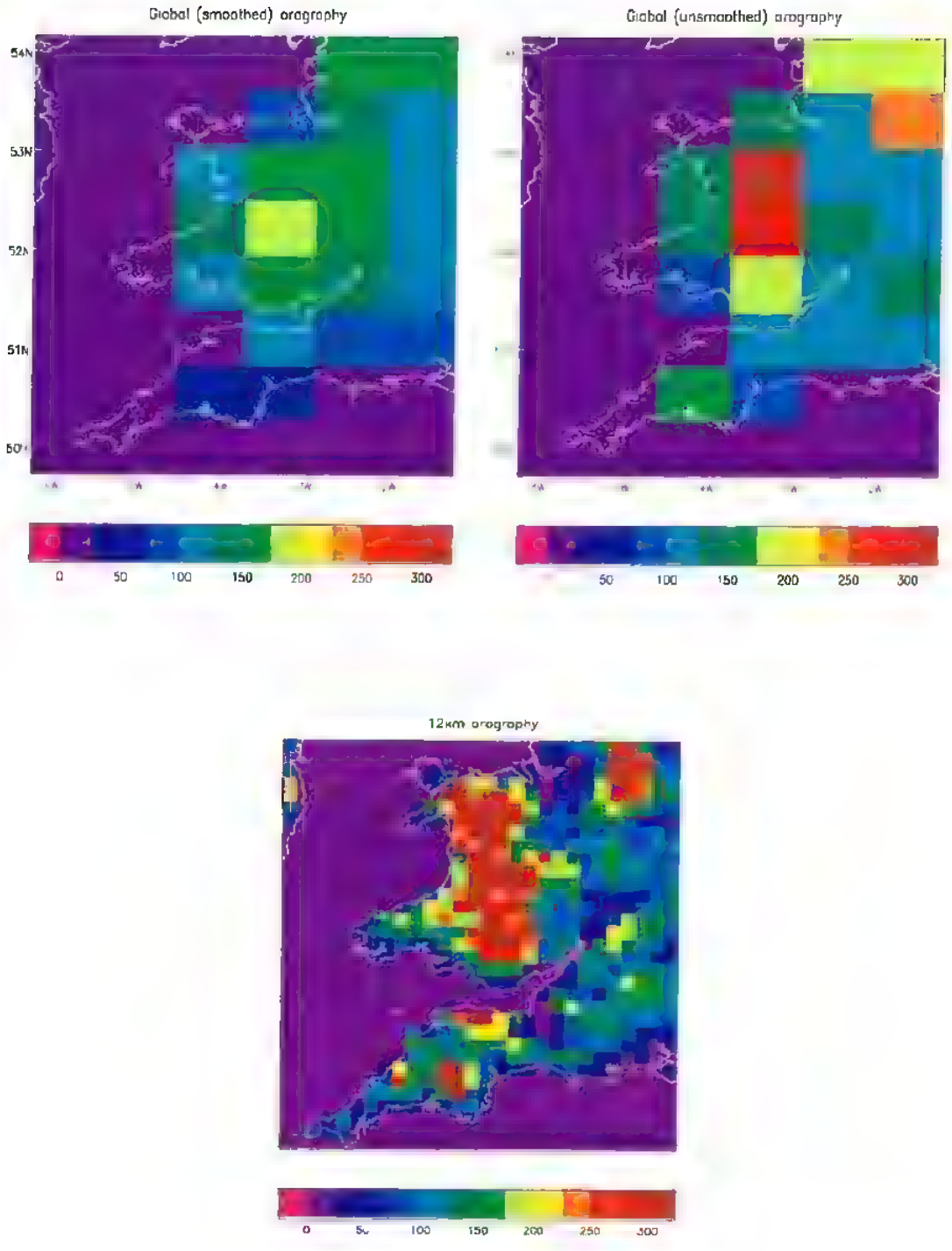

Figure 29 Comparison of global model smoothed and unsmoothed orography and 12km orography. Coastlines shown are for location purposes only and are more detailed than used by models. The colour scale has been burnt out at the top in the 12km model in order to clearly show the global orography fields.

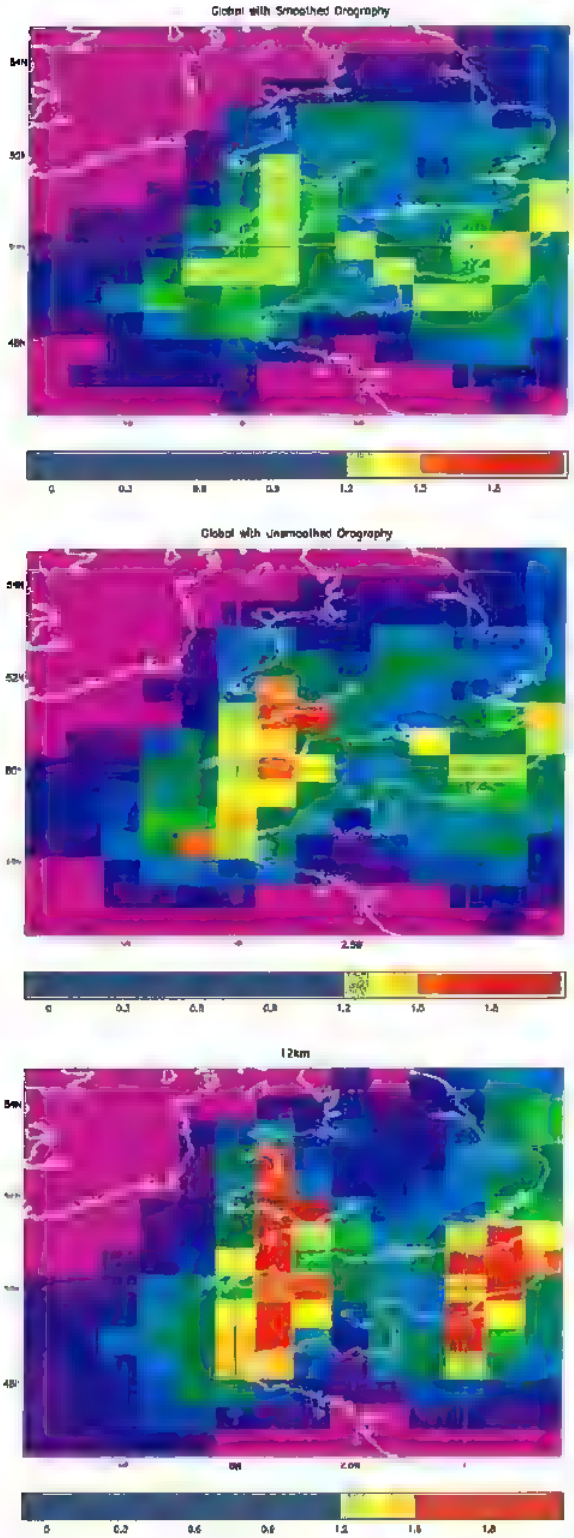

Figure 30. 11-12Z Accumulated rainfall from the global and 12km models.

Current JCMM Internal reports

This series of JCMM Internal Reports, initiated in 1993, contains unpublished reports and also versions of articles submitted for publication. The completed set of Internal Reports is available from the National Meteorological Library on loan, if required.

JCMM Internal Report No	Research strategy and programme		
1	K A Browning et al		
January 1993			

JCMM Internal Report No	The GEWEX Cloud System Study (GCSS) GEWEX Cloud System Science Team		
2			
January 1993			

JCMM Internal Report No	Evolution of a mesoscale upper tropospheric vorticity maximum and comma cloud from a cloud-free two dimensional potential vorticity anomaly		
3	K A Browning		
January 1993			

JCMM Internal Report No	The global energy and water cycle		
4	K A Browning		
July 1993			

JCMM Internal Report No	Structure of a midlatitude cyclone before occlusion		
5	K A Browning	N Roberts	
July 1993			

JCMM Internal Report No	Developments in systems and tools for weather forecasting		
6	K A Browning	G Szejwach	
July 1993			

JCMM Internal Report No	Diagnostic study of a narrow cold frontal rainband and severe winds associated with a stratospheric intrusion		
7	K A Browning	R Reynolds	
August 1993			

JCMM Internal Report No	Survey of perceived priority issues in the parametrizations of cloud-related processes in GCMs		
8	K A Browning		
September 1993			

JCMM Internal Report No	The effect of rain on longwave radiation		
9	I Dharssi		
September 1993			

JCMM Internal Report No	Cloud microphysical processes - a description of the parametrization used in the large eddy model		
10	H Swann		
October 1993			

JCMM Internal Report No	An appreciation of the meteorological research of Ernst Kleinschmidt		
11	A J Thorpe		
May 1992			

JCMM Internal Report No	Potential vorticity of flow along the Alps		
12	A J Thorpe	H Volkert	D Heimann
August 1992			

JCMM Internal Report No	The representation of fronts		
13	A J Thorpe		
January 1993			

JCMM Internal Report No	A parametrization scheme for symmetric instability: test for an idealised flow		
14	A J Thorpe	C S Chan	
February 1993			

Current JCMM Internal reports

This series of JCMM Internal Reports, initiated in 1993, contains unpublished reports and also versions of articles submitted for publication. The completed set of Internal Reports is available from the National Meteorological Library on loan, if required.

JCMM Internal Report No **15** — **The Fronts 92 Experiment: a Quicklook Atlas**

T D Hewson

November 1993

JCMM Internal Report No **16** — **Frontal wave stability during moist deformation frontogenesis Part 1: Linear wave dynamics**

A J Thorpe C H Bishop

May 1993

JCMM Internal Report No **17** — **Frontal wave stability during moist deformation frontogenesis Part 2. The suppression of non-linear wave development**

A J Thorpe C H Bishop

May 1993

JCMM Internal Report No **18** — **Gravity waves in sheared ducts**

A J Thorpe S Moinserrat

October 1993

JCMM Internal Report No **19** — **Potential vorticity and the electrostatics analogy: quasi-geostrophic theory**

A J Thorpe C H Bishop

November 1993

JCMM Internal Report No **20** — **Recent advances in the measurement of precipitation by radar**

A J Illingworth

April 1993

JCMM Internal Report No **21** — **Micro-physique et givrage: cloud microphysics and aircraft icing**

A J Illingworth

May 1993

JCMM Internal Report No **22** — **Differential phase measurements of precipitation**

A J Illingworth M Blackman

May 1993

JCMM Internal Report No **23** — **Estimation of effective radius of cloud particles from the radar reflectivity**

A J Illingworth N I Fox

May 1993

JCMM Internal Report No **24** — **A simple method of Dopplerising a pulsed magnetron radar**

A J Illingworth A Hua J Eastment

November 1993

JCMM Internal Report No **25** — **Radiation and polar lows**

G C Craig

February 1994

JCMM Internal Report No **26** — **Collected preprints submitted to the International Symposium on the Life Cycles of Extratropical Cyclones; Bergen, Norway, 27 June - 1 July 1994**

April 1994

JCMM Internal Report No **27** — **Convective frontogenesis**

A J Thorpe D J Parker

April 1994

JCMM Internal Report No **28** — **Improved measurement of the ice water content in cirrus using a total water evaporator**

P R A Brown P N Francis

April 1994

Current JCMM Internal reports

This series of JCMM Internal Reports, initiated in 1993, contains unpublished reports and also versions of articles submitted for publication. The completed set of Internal Reports is ava lable from the National Meteorological Library on loan, if required.

JCMM Internal Report No	Mesoscale effects of a dry intrusion within a vigorous cyclone				
29	K A Browning	B W Golding			
April 1994					
JCMM Internal Report No	GEWEX Cloud System Study, Science Plan				
30					
May 1994					
JCMM Internal Report No	Parametrization of momentum transport by convectively generated gravity waves				
31	R Kershaw				
May 1994					
JCMM Internal Report No	Mesoscale Modelling Newsletter No 5				
32					
May 1994					
JCMM Internal Report No	Observations of the mesoscale sub-structure in the cold air of a developing frontal cyclone				
33	K A Browning	N Roberts	S A Clough	C S A Davitt	T D Hewson
May 1994					
JCMM Internal Report No	Longwave radiative forcing of a simulated tropical squall line				
34	I Dharssi				
July 1994					
JCMM Internal Report No	On the nature of the convective circulation at a kata-cold front				
35	K A Browning				
September 1994					
JCMM Internal Report No	Collective preprints of papers submitted to the COST-75 International Seminar on Advanced Weather Radar Systems, Brussels, 20-23 September 199				
36					
November 1994					
JCMM Internal Report No	Use of satellite imagery to diagnose events leading to frontal thunderstorms: Parts I and II of a case study				
37	K A Browning	N Roberts			
November 1994					
JCMM Internal Report No	The role of spaceborne millimetre-wave radar in the global monitoring of ice cloud				
38	K A Browning	A J Illingworth	A J Heymsfield	G M McFarquhar	M Gosset
December 1994					
JCMM Internal Report No	Potential vorticity inversion				
39	M Ziemianski				
October 1994					
JCMM Internal Report No	Theory of mature tropical cyclones; a comparison between Kleinschmidt (1951) and Emanuel (1986)				
40	S L Gray				
December 1994					
JCMM Internal Report No	Dispersion and removal of pollutants during the passage of an atmospheric frontal system				
41	N R Gimson				
December 1994					
JCMM Internal Report No	The role of snow sublimation in frontogenesis				
42	A J Thorpe	D J Parker			
December 1994					

Current JCMM Internal reports

This series of JCMM Internal Reports, initiated in 1993, contains unpublished reports and also versions of articles submitted for publication. The completed set of Internal Reports is available from the National Meteorological Library on loan, if required.

JCMM Internal Report No **43** — **Potential vorticity and the electrostatics Analogy: Ertel-Rossby formulation**
A J Thorpe C H Bishop
December 1994

JCMM Internal Report No **44** — **Mesoscale aspect of extratropical cyclones: an observational perspective**
K A Browning
January 1995

JCMM Internal Report No **45** — **A polar low outbreak: evolution and mesoscale structures**
G C Craig T D Hewson C Claud
February 1995

JCMM Internal Report No **46** — **Generation of near-surface gusts of deep convection**
R Kershaw K Nakamura
April 1995

JCMM Internal Report No **47** — **Attribution concepts applied to the Omega Equation**
A J Thorpe S A Clough C S A Davitt
June 1995

JCMM Internal Report No **48** — **Parametrization of mixed-phase cloud and precipitation**
S P Ballard M G Hutchinson
June 1995

JCMM Internal Report No **49** — **Short-range forecasting of stratocumulus: initialization prediction**
S P Ballard S D Jackson B Macpherson
June 1995

JCMM Internal Report No **50** — **Contributions of the JCMM/Dept of Meteorology Radar Group to the 27th AMS Radar Meteorology Conference, Vail October 1995**
June 1995

JCMM Internal Report No **51** — **Cold pools in shear**
D J Parker
September 1995

JCMM Internal Report No **52** — **High-resolution analysis of frontal fracture**
K A Browning S P Ballard C S A Davitt
September 1995

JCMM Internal Report No **53** — **The albedo of broken cloud fields: calculations using a modified two stream radiation code**
I Dharssi R Kershaw
October 1995

JCMM Internal Report No **54** — **Parametrization of momentum transport by convection. I: theory and cloud modelling results**
R Kershaw D Gregory
November 1995

JCMM Internal Report No **55** — **Variation of frontal structure along a cold front**
K A Browning N M Roberts
November 1995

JCMM Internal Report No **56** — **Secondary frontal waves**
D Parker
December 1995

Current JCMM Internal reports

This series of JCMM Internal Reports, initiated in 1993, contains unpublished reports and also versions of articles submitted for publication. The completed set of Internal Reports is available from the National Meteorological Library on loan, if required.

JCMM Internal Report No	Objective fronts				
57	T D Hewson				
March 1996					
JCMM Internal Report No	Mesoscale analysis of the activation of a cold front during cyclogenesis				
58	K A Browning	N M Roberts	T D Hewson		
June 1996					
JCMM Internal Report No	Investigation of different representations of rain in a 1-d evaporation model				
59	H Swann				
May 1996					
JCMM Internal Report No	Parametrization of diabatic processes in the inversion of the omega-equation				
60	A J Thorpe	M Athanassiadou			
June 1996					
JCMM Internal Report No	The role of the environmental flow in the development of secondary frontal cyclones				
61	A J Thorpe	I A Renfrew	A Joly		
June 1996					
JCMM Internal Report No	Consequences of the geostrophic momentum approximation on barotropic instability				
62	A J Thorpe	A Joly	S Malardel		
June 1996					
JCMM Internal Report No	Contributions to the AMS/RMS Conference on Mesoscale Processes				
63					
9-13 September 1996					
JCMM Internal Report No	Vorticity and potential vorticity in stratified flows interacting with an isolated obstacle				
64	A J Thorpe	J A Gutierrez			
September 1996					
JCMM Internal Report No	Triple point development: two case studies				
65	D Parker				
September 1996					
JCMM Internal Report No	Radar observations of wind-shear splitting within evolving atmospheric Kelvin-Helmholtz billows				
66	K A Browning	D Chapman			
April 1997					
JCMM Internal Report No	Cold frontal structure derived from radar wind profilers				
67	K A Browning	N M Roberts	D Jerret	J Nash	T Oakley
May 1997					
JCMM Internal Report No	The dry intrusion and its effect on the frontal, cloud and precipitation structure of extratropical cyclones				
68	K A Browning				
22 May 1997					
JCMM Internal Report No	Met. Office Unified Model data, diagnostics, graphics programs, and other observational data available from the JCMM through the aegis of the universities				
69	P Panagi	E Dicks			
June 1997					
JCMM Internal Report No	Contributions of the JCMM/Dept of Meteorology Radar Group to the 28th AMS Radar Meteorology Conference				
70					
September 1997					

Current JCMM Internal reports

This series of JCMM Internal Reports, initiated in 1993, contains unpublished reports and also versions of articles submitted for publication. The completed set of Internal Reports is available from the National Meteorological Library on loan, if required.

JCMM Internal Report No **71** — **Sensitivity of short-range weather forecasts to local potential vorticity modifications**

A J Thorpe M Demirtas

July 1997

JCMM Internal Report No **72** — **Objective identification of frontal wave cyclones**

T D Hewson

August 1997

JCMM Internal Report No **73** — **Attribution and its application to mesoscale structure associated with tropopause folds**

A J Thorpe

September 1997

JCMM Internal Report No **74** — **The role of the environmental flow in the development of secondary frontal cyclones**

A J Thorpe I A Renfrew C H Bishop

September 1997

JCMM Internal Report No **75** — **Potential vorticity: a short history of its definitions and uses**

A J Thorpe H Volkert

September 1997

JCMM Internal Report No **76** — **Superposing semi-geostrophic potential vorticity anomalies**

A J Thorpe H R Birkett

September 1997

JCMM Internal Report No **77** — **Short period forecasting of catchment-scale precipitation. Part 1: the role of Numerical Weather Prediction**

A J Thorpe M A Pedder M Haile

September 1997

JCMM Internal Report No **78** — **Verification of the tracking technique used in an experimental cloud motion wind inferring system**

K A Browning Z Wang G A Kelly

October 1997

JCMM Internal Report No **79** — **A preliminary study of Fourier series analysis for cloud tracking with GOES high temporal resolution images**

Z Wang

October 1997

JCMM Internal Report No **80** — **Analysis of an ex tropical cyclone after reintensifying as a warm-core extratropical cyclone**

K A Browning P Panagi G Vaughan

November 1997

JCMM Internal Report No **81** — **A JCMM overview of FASTEX IOPs**

S A Clough H W Lean N M Roberts H Birkett J P Chaboureau R Dixon M Griffiths T D Hewson A Montani

January 1998

JCMM Internal Report No **82** — **Programs for PV inversion and modification**

M Demirtas

December 1997

JCMM Internal Report No **83** — **Release of potential shearing instability in warm frontal zones**

K A Browning D Chapman

February 1998

JCMM Internal Report No **84** — **The European Cloud-Resolving Modelling Programme (EUCREM)**

P W White

April 1998

Current JCMM Internal reports

This series of JCMM Internal Reports, initiated in 1993, contains unpublished reports and also versions of articles submitted for publication. The completed set of Internal Reports is available from the National Meteorological Library on loan, if required.

JCMM Internal Report No	**A frontal wave database**			
85	T D Hewson			
April 1998				
JCMM Internal Report No	**Layering observed in dropsoundings from IOP 1 of Fronts 92**			
86	S A Clough			
May 1998				
JCMM Internal Report No	**Use of wind-shear displays for Doppler radar data**			
87	K A Browning	D Chapman		
May 1998				
JCMM Internal Report No	**Radar estimates of rainfall rates at the ground in bright band and non-bright band events**			
88	T J Smyth	A J Illingworth		
June 1998				
JCMM Internal Report No	**Correction for attenuation of radar reflectivity using polarisation data**			
89	A J Illingworth	T J Smyth		
June 1998				
JCMM Internal Report No	**The effects of convection on chemical reactions and precipitation scavenging**			
90	N R Gimson			
July 1998				
JCMM Internal Report No	**How to use the display program DISP**			
91	N M Roberts			
August 1998				
JCMM Internal Report No	**Conceptual models of cyclogenesis**			
92	A T Semple			
August 1998				
JCMM Internal Report No	**Observations of oblate hail using dual polarisation radar and implications for hail detection schemes**			
93	A J Illingworth	T J Smyth	T M Blackman	
September 1998				
JCMM Internal Report No	**The semigeostrophic diagnosis of vertical motion. Part I: Formulation and co-ordinate transformations**			
94	A J Thorpe	M A Pedder		
September 1998				
JCMM Internal Report No	**The semigeostrophic diagnosis of vertical motion. Part II: Results for an idealised baroclinic wave life cycle**			
95	A J Thorpe	M A Pedder		
September 1998				
JCMM Internal Report No	**Convective destabilisation by a tropopause fold diagnosed using potential vorticity inversion**			
96	K A Browning	A J Thorpe	M Griffiths	
October 1998				
JCMM Internal Report No	**Forecast skill of the ECMWF model using targeted observations during FASTEX**			
97	A J Thorpe	A Montani	R Buizza	P Unden
October 1998				
JCMM Internal Report No	**Observations and model simulations of the FASTEX IOP 16 frontal wave - effects of sublimation**			
98	S A Clough	H W Lean	N M Roberts	R M Forbes
December 1998				

Current JCMM Internal reports

This series of JCMM Internal Reports, initiated in 1993, contains unpublished reports and also versions of articles submitted for publication. The completed set of Internal Reports is available from the National Meteorological Library on loan, if required.

JCMM Internal Report No	**The application of conceptual models in NWP**					
99	A T Semple					
January 1999						
JCMM Internal Report No	**Mesoscale analysis of arc rainbands in a dry slot**					
100	K A Browning	N M Roberts				
January 1999						
JCMM Internal Report No	**Interaction of mesoscale tropopause depressions with a warm-core cyclone: observational and model analyses, and sensitivity to analysis error**					
101	K A Browning	A J Thorpe	A Montani	D Parsons	M Griffiths	
February 1999	P Panagi	E M Dicks				
JCMM Internal Report No	**The use of water vapour imagery and PV inversion to adjust initial conditions in NWP**					
102	S J Swarbrick					
February 1999						
JCMM Internal Report No	**Summary notes for a lecture course on Waves in the Atmosphere and Ocean**					
103	A A White					
March 1999						
JCMM Internal Report No	**Results of a questionnaire on the operational value of conceptual models (CMs) of fronts and cyclones**					
104	N M Roberts	M V Young				
July 1999						
JCMM Internal Report No	**Contributions to the Poster Session at the 1998 UWERN Annual Science Meeting**					
105	A A White					
August 1999						
JCMM Internal Report No	**The objective analysis of dropsonde data from FASTEX**					
106	S A Clough	N M Roberts	R M Forbes	M Dixon	A Macallan	
January 2000						
JCMM Internal Report No	**Implications for Mesoscale Modelling from a Study of the FASTEX IOP 16 Mid-latitude Cyclone**					NWP Technical Report No 302
107	P A Clark	N M Roberts	R M Forbes	H W Lean		
March 2000						
JCMM Internal Report No	**The use of water vapour imagery and PV inversion to adjust initial conditions in NWP**					NWP Technical Report No 291
108	S J Swarbrick					
September 1999						
JCMM Internal Report No	**A guide to aspects of water vapour imagery interpretation: the significance of dry regions**					NWP Technical Report No 294
109	N M Roberts					
January 2000						
JCMM Internal Report No	**The relationship between water vapour imagery and thunderstorms**					NWP Technical Report No 300
110	N M Roberts					
February 2000						
JCMM Internal Report No	**Holomorphic structures in hydrodynamical models of nearly geostrophic flow**					NWP Technical Report No 293
111	I Roulstone	V N Roubtsov				
January 2000						
JCMM Internal Report No	**Multi-sensor synthesis of the mesoscale structure of a cold-air comma cloud system**					NWP Technical Report No 301
112	K A Browning	P Panagi	E M Dicks			
March 2000						

Current JCMM Internal reports

This series of JCMM Internal Reports, initiated in 1993, contains unpublished reports and also versions of articles submitted for publication. The completed set of Internal Reports is available from the National Meteorological Library on loan, if required.

JCMM Internal Report No	**Observations of stratospheric air entering the circulation of a polar low**			NWP Technical Report No 307
113	K A Browning	E M Dicks		
May 2000				
JCMM Internal Report No	**Wind profiler – Unified Model comparison statistics**			NWP Technical Report No 309
114	P Panagi	E M Dicks		
March 2000				
JCMM Internal Report No	**Towards a similarity theory of moist convective updrafts**			NWP Technical Report No 310
115	G C Craig	O Stiller		
May 2000				
JCMM Internal Report No	**The mystery of striated cloud heads in satellite imagery**			NWP Technical Report No 312
116	K A Browning	R S Dixon	G J Shutts	
April 2000				
JCMM Internal Report No	**MDIAG: a Fortran 90 program to compute diagnostics on pressure levels from Unified Model data on model levels**			NWP Technical Report No 313
117	P Panagi			
June 2000				
JCMM Internal Report No	**Rearrangements of functions with applications to meteorology and ideal fluid flow**			NWP Scientific Paper No 56
118	R J Douglas			
June 2000				
JCMM Internal Report No	**Tests of New Dynamics Model on the FASTEX IOP16 case**			NWP Technical Report No 320
119	H W Lean			
September 2000				
JCMM Internal Report No	**A classification of FASTEX cyclones using a height-attributable QG vertical motion diagnostic**			NWP Scientific Paper No 57
120	K A Browning	T D Hewson	A C L Deveson	
September 2000				
JCMM Internal Report No	**Measurements of dissipation rate in frontal zones**			NWP Scientific Paper No 59
121	K A Browning	D Chapman		
August 2000				
JCMM Internal Report No	**Not Issued**			NWP Technical Report No 331
122				
JCMM Internal Report No	**A Case Study of High Resolution Fog Forecasts with the New Dynamics**			NWP Technical Report No 337
123	P Clark			
November 2000				
JCMM Internal Report No	**Comparison of ECMWF Winter-Season Cloud Fraction with Radar Derived Values**			NWP Technical Report No 338
124	A J Illingworth	R J Hogan	C Jakob	
January 2001				
JCMM Internal Report No	**Deriving Cloud overlap statistics from radar**			NWP Technical Report No 339
125	A J Illingworth	R J Hogan		
January 2001				
JCMM Internal Report No	**Results from simulations of an organised convective event using the New Dynamics at 12, 4 and 2km resolution.**			NWP Technical Report No 344
126	N M Roberts			
January 2001				

Current JCMM Internal reports

This series of JCMM Internal Reports, initiated in 1993, contains unpublished reports and also versions of articles submitted for publication. The completed set of Internal Reports is available from the National Meteorological Library on loan, if required.

JCMM Internal Report No	**A North Atlantic Survey of Cyclogenesis in 1999: Unified Model Performance in Short Range Forecasts & The Relationship Between Potential Vorticity, Water Vapour Imagery**				NWP Technical Report No 348
127	A Semple				
March 2001					
JCMM Internal Report No	**Are there higher-accuracy analogues of semigeostrophic theory?**				NWP Scientific Paper No 61
128	I Roulstone	M E McIntyre			
June 2001					
JCMM Internal Report No	**Stacked slantwise convective circulations**				NWP Scientific Paper No 62
129	K A Browning	D Chapman	R S Dixon		
April 2001					
JCMM Internal Report No	**A Meteorological Assessment of the Geostrophic Co-ordinate Transform and Error Breeding System when used in 3D Variational Data Assimilation**				NWP Technical Report No 357
130	A Semple				
June 2001					
JCMM Internal Report No	**The dynamics of a mid-latitude cyclone with very strong latent heat release**				NWP Scientific Paper No 63
131	G C Craig	F Ahamdi-Givi			
July 2001					
JCMM Internal Report No	**A Study of the Effects of Horizontal and Vertical Resolution in the New Dynamics representation of FASTEX IOP16**				NWP Scientific Paper No 64
132	H W Lean				
October 2001					
JCMM Internal Report No	**Modelling Low Level Winds with the Met Office New Dynamics Model**				NWP Scientific Paper No 66
133	R A Capon				
9 May 2002					
JCMM Internal Report No	**Layer-wise attribution of vertical motion and the influence of potential-vorticity anomalies on synoptic development**				NWP Scientific Paper No 67
134	K A Browning	A J Thorpe	M Dixon		
May 2002					
JCMM Internal Report No	**The sting at the end of the tail: damaging winds associated with extratropical cyclones. Part I: observational evidence and proposed mechanisms**				NWP Technical Report No 388
135	K A Browning				
July 2002					
JCMM Internal Report No	**Simulation of Orographic Rainfall in South Wales with UM Version 5.2**				NWP Scientific Report 70
136	H W Lean				
July 2002					

Met Office Joint Centre for Mesoscale Meteorology Department of Meteorology
University of Reading PO Box 243 Reading RG6 6BB United Kingdom
Tel: +44 (0)118 931 8425 Fax: +44 (0)118 931 8791
www.metoffice.com